Geometrical differences in target volumes between slow CT and 4D CT imaging in stereotactic body radiotherapy for lung tumors in the upper and middle lobe

Mitsuhiro Nakamura, Yuichiro Narita,[a] Yukinori Matsuo, and Masaru Narabayashi
Department of Radiation Oncology and Image-applied Therapy, Graduate School of Medicine, Kyoto University, Kyoto 606-8507, Japan

Manabu Nakata and Shinsuke Yano
Clinical Radiology Service Division, Kyoto University Hospital, Kyoto 606-8507, Japan

Yuki Miyabe, Kiyotomo Matsugi, Akira Sawada, Yoshiki Norihisa, and Takashi Mizowaki
Department of Radiation Oncology and Image-applied Therapy, Graduate School of Medicine, Kyoto University, Kyoto 606-8507, Japan

Yasushi Nagata
Division of Radiation Oncology, Hiroshima University Hospital, Hiroshima 734-0037, Japan

Masahiro Hiraoka
Department of Radiation Oncology and Image-applied Therapy, Graduate School of Medicine, Kyoto University, Kyoto 606-8507, Japan

(Received 19 March 2008; revised 7 July 2008; accepted for publication 16 July 2008; published 19 August 2008)

Since stereotactic body radiotherapy (SBRT) was started for patients with lung tumor in 1998 in our institution, x-ray fluoroscopic examination and slow computed tomography (CT) scan with a rotation time of 4 s have been routinely applied to determine target volumes. When lung tumor motion observed with x-ray fluoroscopy is larger than 8 mm, diaphragm control (DC) is used to reduce tumor motion during respiration. After the installation of a four-dimensional (4D) CT scanner in 2006, 4D CT images have been supplementarily acquired to determine target volumes. It was found that target volumes based on slow CT images were substantially different from those on 4D CT images, even for patients with lung tumor motion no larger than 8 mm. Although slow CT scan might be expected to fare well for lung tumors with motion range of 8 mm or less, the potential limitations of slow CT scan are unknown. The purpose of this study was to evaluate the geometrical differences in target volumes between slow CT and 4D CT imaging for lung tumors with motion range no larger than 8 mm in the upper and middle lobe. Of the patients who underwent SBRT between October 2006 and April 2008, 32 patients who had lung tumor with motion range no larger than 8 mm and did not need to use DC were enrolled in this study. Slow CT and 4D CT images were acquired under free breathing for each patient. Target volumes were manually delineated on slow CT images ($TV_{slow\ CT}$). Gross tumor volumes were also delineated on each of the 4D CT volumes and their union ($TV_{4D\ CT}$) was constructed. Volumetric and statistical analyses were performed for each patient. The mean ± standard deviation (S.D.) of $TV_{slow\ CT}/TV_{4D\ CT}$ was 0.75 ± 0.17 (range, 0.38–1.10). The difference between sizes of $TV_{slow\ CT}$ and $TV_{4D\ CT}$ was not statistically significant ($P=0.096$). A mean of 8% volume of $TV_{slow\ CT}$ was not encompassed in $TV_{4D\ CT}$ (mean ± S.D. $= 0.92 \pm 0.07$). The patients were separated into two groups to test whether the quality of target delineation on slow CT scans depends on respiratory periods below or above the CT rotation time of 4 s. No significant difference was observed between these groups ($P=0.229$). Even lung tumors with motion range no larger than 8 mm might not be accurately depicted on slow CT images. When only a single slow CT scan was used for lung tumors with motion range of 8 mm or less, 95% confidence values for additional margins for $TV_{slow\ CT}$ to encompass $TV_{4D\ CT}$ were 4.0, 5.4, 4.9, 5.1, 1.8, and 1.7 mm for lateral, medial, ventral, dorsal, cranial, and caudal directions, respectively.
[DOI: 10.1118/1.2968096]

Key words: 4D CT, slow CT, respiratory motion, margin, lung cancer

I. INTRODUCTION

The local control rate of conventional radiotherapy is not satisfactory for lung cancer, even in stage I cases.[1,2] However, since the introduction of stereotactic body radiotherapy (SBRT), higher local control rates comparable to those with surgery have been reported.[3–7] In recent years, guidelines for SBRT have been developed and written collaboratively by the American Society of Therapeutic Radiology and Oncol-

ogy and the American College of Radiology.[8] SBRT is increasingly becoming an important treatment option for stage I lung cancer.

SBRT allows high-dose areas limited to a target volume with a high degree of precision within the body and reduces doses delivered to other areas such as organs at risk. Therefore, target delineation is more crucial in treatment planning of SBRT. While there is an increasing use of multiple imaging modalities, current treatment planning is primarily based on computed tomography (CT). It has been recognized that severe motion artifacts, including axial slices being shuffled out of order and organs being imaged as distinct parts, can sometimes be introduced if organ motion is present during standard CT scan under free breathing.[9–11] Such motion artifacts may give an inaccurate representation of the shape, volume, and position of normal organs and target volumes, and lead to crucial delineation error in treatment planning. Three CT acquisition methods are commonly used to visualize the entire range of respiratory tumor motion on CT images, namely inhale and exhale breath-hold CT scan,[12–14] slow CT scan,[15–17] and four-dimensional (4D) CT scan.[18–22]

In our institution, SBRT was started in 1998 for patients with lung tumor. The eligibility criteria of SBRT for lung tumor in our institution are as follows: (1) tumor diameter is no larger than 4 cm, (2) tumor is located peripherally, and (3) one or two tumors in metastasis cases. X-ray fluoroscopic examination and slow CT scan with a rotation time of 4 s have been routinely applied to determine target volumes. When lung tumor motion observed with x-ray fluoroscopy is larger than 8 mm, a small abdominal pressure plate, called "diaphragm control (DC)," is applied to reduce tumor motion.[23] Additionally, x-ray fluoroscopy is used to determine whether the target volume visualized on slow CT images is sufficiently large to encompass tumor motion. When the target volume on slow CT images is found to be insufficient, we manually correct the target volume based on x-ray fluoroscopy evaluation. Since a four-slice CT scanner which allows 4D CT scan was installed in 2006, 4D CT images have been supplementarily utilized to determine target volumes. We found that target volumes based on slow CT images were substantially different from those based on 4D CT images, even for patients with lung tumor motion no larger than 8 mm. The observed differences need to be quantitatively reflected in treatment planning.

Some researchers compared the difference in target volumes between different CT scan techniques for patients with lung tumors.[16,20,24,25] van Sörnsen de Koste *et al.* and Seki *et al.* showed the effectiveness of the combined use of slow CT and helical CT in the delineation of internal target volume.[16,24] Underberg *et al.* reported that a single 4D CT scan can replace six rapid helical CT scans in defining individualized target volumes for stage I non-small cell lung cancer.[20] Bradley *et al.* compared helical CT, maximum intensity projection, and averaged intensity 4D CT images to determine the best CT-based volume definition method for encompassing tumor motion within the planning target volume (PTV) for SBRT in stage I lung cancer.[25] However, the comparison of the target volumes based on slow CT scan with those based on 4D CT scan has not yet been reported. The potential limitations of slow CT scan are also unknown, although slow CT scan might be expected to fare well for lung tumors with motion range of 8 mm or less. The purpose of this study was to evaluate the geometrical differences in target volumes between slow CT and 4D CT imaging for lung tumors with motion range no larger than 8 mm in the upper and middle lobe.

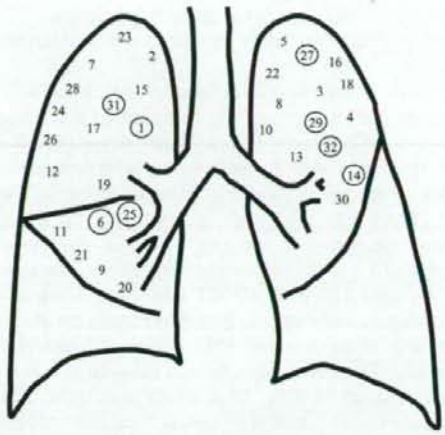

FIG. 1. Diagram of lung tumor location for each patient. Numbers represent case numbers. Lung tumors were peripherally located in the right upper lobe (12 patients), in the right middle lobe (6 patients), and in the left upper lobe (14 patients). Data of the circled numbers are shown in Tables I and II.

II. MATERIALS AND METHODS

II.A. Patients

Of the patients who underwent SBRT between October 2006 and April 2008, 32 patients who had lung tumor with motion range no larger than 8 mm and did not need to use DC after x-ray fluoroscopic evaluation were enrolled in this study. If DC was required to limit respiratory motion, reliable motion signals could not be acquired for 4D CT data acquisition and therefore these patients were excluded from this study. Twenty-three men and nine women with a median age of 74 years (range, 56–87 years) were included. Lung tumors were located in the right upper lobe (12 patients), in the right middle lobe (6 patients), and in the left upper lobe (14 patients) (Fig. 1). Written informed consent for SBRT was obtained from each patient before treatment planning.

II.B. X-ray fluoroscopic evaluation and CT data acquisition

Before CT data acquisition, the patient was fixed in a stereotactic body frame (SBF) (Elekta Corp., Stockholm, Sweden) with their arms raised using a vacuum pillow.[23,26] The patient was asked to breathe regularly and quietly by radiological technicians. Respiratory tumor motion was then observed with an x-ray simulator (Acuity; Varian Medical

Systems, Palo Alto, CA) from orthogonal directions. DC was applied to reduce lung tumor motion when it was larger than 8 mm.[23]

After x-ray fluoroscopic evaluation, the patient immobilized with SBF was placed on the couch of a CT scanner (LightSpeed RT; General Electric Medical Systems, Waukesha, WI). First, slow CT scan was routinely performed. CT slices were sequentially acquired from the lower neck to the upper abdomen in axial mode. The CT slice thickness and rotation time were 1.25 mm and 4 s around the tumor and 2.5 mm and 1 s in the other areas, respectively. Immediately after the slow CT scan, 4D CT data were acquired only around an area including the lung tumor using the Real-time Positioning Management (RPM) system (Varian) in axial cine mode.[18–22] Cine duration time of the scan at each couch position was set to 6 or 7.5 s, which was more than the maximum observed respiratory period. Cine interval between images was 0.5 s. With these settings, we usually obtain approximately 12–15 images per couch position. To prevent marker vibration resulting from couch movement, interscan delay was set to longer than 2 s. CT data were reconstructed in a field of view of 520 mm on a 512×512 grid for both CT scans. The RPM system illuminated and tracked an infrared reflective marker placed on the patient's abdomen. RPM software calculated the respiratory phase at each instant in time based on modeling the abdominal motion amplitude. Motion phases were assigned for each respiratory phase in percent values, end-inhalation corresponding to 0% and end-exhalation to 50%. After 4D CT scan, all 4D CT slices and respiratory motion data were transferred to an Advantage 4D workstation (GE), and Advantage 4D software retrospectively sorted the images into eight respiratory phase bins.

II.C. Target volume definition

All CT datasets were imported into a commercial three-dimensional radiation planning system (Eclipse 7.3.10; Varian), and thereafter slow CT images and 4D CT images were superimposed using the same coordinate origin that they shared. Alignment of bony structures was reviewed by one medical physicist (M.N.) on subtraction images to check the patient's movement between slow CT scan and 4D CT scan. Target volumes were delineated on the Eclipse using lung CT window setting [window width: 2000 Hounsfield units (HU) and window level: -700 HU]. To eliminate inter-observer variations,[27–29] target volumes were manually contoured by the same medical physicist (M.N.) on slow CT scan images as well as 4D CT images. All contours were reviewed by one experienced radiation oncologist (Y.M.). The definitions of all different target volumes generated were as follows.

- $GTV_{T\%}$: Gross tumor volume (GTV) delineated on T% phase of 4D CT images. Each $GTV_{T\%}$ was defined without reference to previously contoured GTVs.
- $TV_{4D\ CT}$: Target volume derived from contouring GTVs on all eight phases of the 4D CT. $TV_{4D\ CT}$ was defined as follows:

$$TV_{4D\ CT} = GTV_{0\%} \cup GTV_{12\%} \cup \cdots \cup GTV_{87\%}.$$

- $TV_{slow\ CT}$: Target volume derived from slow CT scan. $TV_{slow\ CT}$ included a blurred area surrounding the tumor. The area indicated respiratory motion.
- TV_{COM}: Target volume defined as an overlapping volume between $TV_{slow\ CT}$ and $TV_{4D\ CT}$. TV_{COM} was defined as follows:

$$TV_{COM} = TV_{slow\ CT} \cap TV_{4D\ CT}.$$

II.D. Analysis

From 4D CT datasets, volumetric variations in GTVs for each patient were analyzed. The coefficient of variation (C.V.) was employed to evaluate variations in the GTV size because of motion artifacts and tumor deformation during respiration.[22] Intrafractional motion range of the GTVs was also measured in the right-left (RL), anterior-posterior (AP), and cranial-caudal (CC) directions.

The size and centroid shift between $TV_{slow\ CT}$ and $TV_{4D\ CT}$ were compared for all patients. When $TV_{slow\ CT}$ is fully covered by $TV_{4D\ CT}$, TV_{COM} is equal to $TV_{slow\ CT}$. In order to test whether slow CT scan with a rotation time of

TABLE I. Volumetric variations and motion range of GTVs as well as the averaged breathing period for patients with 3D GTV centroid motion range larger than 4.4 mm corresponding to the 75th percentile. *Abbreviations:* GTV=gross tumor volume; Avg.=average; S.D.=standard deviation; C.V.=coefficient of variation; RL=right-left; AP=anterior-posterior; CC=cranial-caudal; $3D=\sqrt{RL^2+AP^2+CC^2}$.

	GTV			Motion range (mm)				Averaged breathing period (s)
Case	Avg. (ml)	S.D. (ml)	C.V. (%)	RL	AP	CC	3D	
1	2.11	0.13	6.08	1.3	3.6	5.8	6.9	5.63
6	1.45	0.13	8.99	3.9	4.5	1.4	6.1	4.27
14	3.99	0.27	6.77	0.8	4.2	4.9	6.5	4.38
25	0.56	0.01	2.32	3.0	1.5	7.1	7.9	4.80
27	3.09	0.23	7.44	1.0	2.4	5.5	6.1	3.54
29	4.49	0.26	5.79	1.0	3.2	2.9	4.4	3.66
31	11.73	0.76	6.48	1.9	2.9	2.7	4.4	5.55
32	1.33	0.08	6.02	1.4	3.3	4.1	5.4	3.27

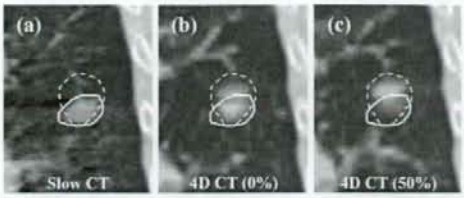

FIG. 2. Coronal images for case 32. Left: slow CT scan. Middle: 0% phase of 4D CT scan. Right: 50% phase of 4D CT scan. Outlines of $TV_{slow\ CT}$ (solid line) and $TV_{4D\ CT}$ (broken line) were overlaid. Additional margins to encompass $TV_{4D\ CT}$ was 0.0, 3.4, 0.6, 5.7, 7.5, and 0.0 mm for lateral, medial, ventral, dorsal, cranial, and caudal directions, respectively.

4 s can capture the motion of a lung tumor in less than 4 s ("<4 sec"), the patients were categorized into a group with a breathing period of "<4 sec" and a group with that of 4 s or longer ("≥4 sec"). The ratio of $TV_{slow\ CT}$ to $TV_{4D\ CT}$ ($TV_{slow\ CT}/TV_{4D\ CT}$) for the two groups was compared.

Maximum distances for lateral-medial, ventral-dorsal, and cranial-caudal directions between $TV_{slow\ CT}$ and $TV_{4D\ CT}$ were measured on anterior-posterior and lateral beam's-eye-view projections. The distances were used to determine the additional margins needed for $TV_{slow\ CT}$ to ensure complete coverage of $TV_{4D\ CT}$ on the Eclipse.

The one-sided Wilcoxon test was performed for statistical analyses. Values of $P<0.05$ were regarded as significant.

III. RESULTS

III.A. 4D CT analysis

The C.V. in GTV volumes ranged from 0.54% to 8.99% with a mean of 3.92% for all cases. The mean ± standard deviation (S.D.) motion ranges were 1.0 ± 0.8, 1.8 ± 1.1, and 2.3 ± 1.7 mm in the RL, AP, and CC directions, respectively. The mean ± S.D. of 3D GTV centroid motion range was 3.3 ± 1.9 mm (range, 0.5–7.9 mm). The breathing period in patients ranged from 2.40 to 6.80 s with a mean ± S.D. of 4.19 ± 0.98 s. Table I shows volumetric variations and motion range of GTVs as well as the averaged breathing period for the patients with 3D GTV centroid motion range larger than 4.4 mm corresponding to the 75th percentile. The maximum C.V. is included in Table I.

III.B. Target volume analysis

Misalignment of bony structures that greatly affected the subsequent results was not seen in any cases. Although the patients did not move between slow CT scan and 4D CT scan, the size and centroid of $TV_{slow\ CT}$ differed from those of $TV_{4D\ CT}$ (Fig. 2). The mean ± S.D. sizes of $TV_{slow\ CT}$ and $TV_{4D\ CT}$ were 6.41 ± 5.70 ml (range, 0.26–24.35 ml) and 8.02 ± 6.21 ml (range, 0.35–24.66 ml), respectively. The mean ± S.D. of $TV_{slow\ CT}/TV_{4D\ CT}$ was 0.75 ± 0.17 (range, 0.38–1.10). The size of $TV_{slow\ CT}$ was smaller than that of $TV_{4D\ CT}$ except in case 4. The difference between the sizes of $TV_{slow\ CT}$ and $TV_{4D\ CT}$ was not statistically significant ($P=0.096$). The mean ± S.D. of centroid shift between $TV_{slow\ CT}$ and $TV_{4D\ CT}$ was 1.5 ± 1.0 mm (range, 0.4–4.8 mm). The mean ± S.D. of $TV_{COM}/TV_{slow\ CT}$ was 0.92 ± 0.07. Table II summarizes the results of $TV_{slow\ CT}$, $TV_{4D\ CT}$, and TV_{COM} for the same patients as in Table I. The minimum $TV_{slow\ CT}/TV_{4D\ CT}$ and the maximum centroid shift are included in Table II. The mean ± S.D. of the breathing periods for the groups of "<4 sec" (14 patients, 43.75%) and "≥4 sec" (18 patients, 56.25%) were 3.32 ± 0.45 s and 4.87 ± 0.69 s, respectively. By comparing $TV_{slow\ CT}/TV_{4D\ CT}$ between the group of "<4 sec" and that of "≥4 sec," the quartile deviation of $TV_{slow\ CT}/TV_{4D\ CT}$ for the group of "<4 sec" was smaller than for the group of "≥4 sec" (Fig. 3). No significant difference was observed between these groups ($P=0.229$).

III.C. Estimation of additional margins

The margins required for $TV_{slow\ CT}$ to encompass $TV_{4D\ CT}$ are shown in Fig. 4. A large variation of margins in each direction was observed among patients. Fifteen patients did not require an additional margin in either the cranial or caudal direction. When only a single slow CT scan was used for treatment planning, 95% confidence values for the addi-

TABLE II. Summary table of $TV_{slow\ CT}$, $TV_{4D\ CT}$, and TV_{COM} for the same patients as in Table I. *Abbreviations:* S.D.=standard deviation; RL=right-left; AP=anterior-posterior; CC=cranial-caudal; $3D=\sqrt{RL^2+AP^2+CC^2}$. *Note:* For centroid shift, a positive value indicates that the centroid of $TV_{4D\ CT}$ is larger than that of $TV_{slow\ CT}$.

						Centroid shift (mm)			
Case	$TV_{slow\ CT}$ (ml)	$TV_{4D\ CT}$ (ml)	TV_{COM} (ml)	$TV_{slow\ CT}/TV_{4D\ CT}$	$TV_{COM}/TV_{slow\ CT}$	RL	AP	CC	3D
1	1.70	4.38	1.68	0.39	0.99	1.1	0.5	0.9	1.5
6	2.20	2.68	1.82	0.82	0.83	1.0	−0.8	1.6	2.0
14	4.10	6.47	3.62	0.63	0.88	−1.2	3.0	1.4	3.5
25	0.49	1.29	0.48	0.38	0.98	−1.1	−1.0	−0.2	1.5
27	4.46	5.46	3.98	0.82	0.89	−0.2	1.8	−0.4	1.9
29	7.49	8.88	6.44	0.84	0.86	−0.2	2.3	−1.3	2.6
31	12.02	18.58	11.67	0.65	0.97	−0.5	0.6	−1.6	1.8
32	1.04	2.45	0.8	0.42	0.77	−0.8	1.3	4.5	4.8

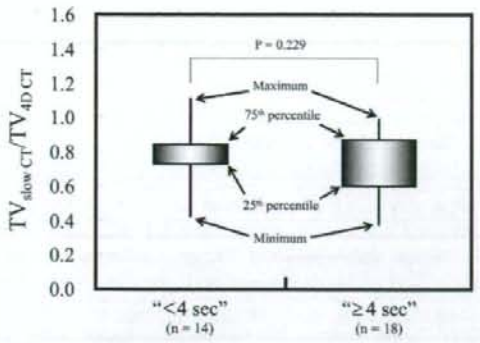

FIG. 3. Comparison of $TV_{slow\ CT}/TV_{4D\ CT}$ for the group of "<4 sec" with that for the group of "≥4 sec" using boxplot. No significant difference was observed between these groups (P=0.229).

tional margin to encompass $TV_{4D\ CT}$ were 4.0, 5.4, 4.9, 5.1, 1.8, and 1.7 mm for lateral, medial, ventral, dorsal, cranial, and caudal directions, respectively.

IV. DISCUSSION

In general, 4D CT data are analyzed to determine the mean tumor position and tumor range of motion.[18,19,21,22] However, data reliability is affected in the presence of motion artifacts. Rietzel *et al.* indicated that large deviations in GTV volume were seen in respiratory phases, especially near mid-exhalation and mid-inhalation because of the maximum velocity of the GTV.[21,22] They employed a C.V. as an index to compare variations in GTV sizes between patients who had significantly different mean GTV sizes, and showed the mean C.V. of 8.2% for the lung tumor in the upper lobe. Residual motion artifacts not only cause a C.V. to be larger, but also incorrectly characterize the geometric shape and extent of the organ. If the target volume is properly delineated without any motion artifacts, a C.V. is ideally zero, but this is uncommon because of motion artifacts and tumor deformation. In this study, evident motion artifacts affecting our results were not observed for any patients in movie-loops viewed in sagittal and coronal reconstructions of the 4D CT. In addition, our mean ± S.D. of the C.V. was 3.92 ± 2.39%, which was relatively lower than the results of Rietzel *et al.*[22] From the results of 4D CT analysis, we judged that the volume and centroid of $TV_{4D\ CT}$ could be reliable. While this study presents data for tumors in the upper and middle lung with motion of 8 mm or less only, other investigators reported lung tumor motion without such selection.[30,31] Given this limitation, our results are valid for tumors in the upper and middle lung with motion of 8 mm or less only.

Seppenwoolde *et al.* and Chen *et al.* reported that the breathing period in patients with lung cancer was within 4 s for most cases.[30,32] The mean ± S.D. of the breathing period was 4.19 ± 0.98 s, and the breathing period was more than 4 s for 18 patients in this study. van Sörnsen de Koste *et al.* described that most lung tumor mobility with a breathing period of less than 4 s could be captured with a slow CT scan with a rotation time of 4 s.[16] From our results of $TV_{slow\ CT}/TV_{4D\ CT}$ analysis, $TV_{slow\ CT}$ was smaller than $TV_{4D\ CT}$, except in case 4, even if the breathing period was less than 4 s. This means that the slow CT scan did not totally capture the motion of the lung tumor with a period of less than 4 s. For example, an additional margin of 7.5 mm was required in the cranial direction for case 32 with an averaged breathing period of 3.27 s. As shown in Fig. 2, his breathing might intermittently cease in the inhalation phase during slow CT scan. Most patients vary their respiratory pattern in frequency, amplitude, and waveform shape.[30] Therefore, the motion pattern of lung tumors during CT scan might be more important in differentiating $TV_{slow\ CT}$ and $TV_{4D\ CT}$ than the breathing period. Patients should be encouraged to perform reproducible and regular respiration during CT data acquisition.

Lagerwaard *et al.* examined how much margin was needed to ensure target volumes with multiple CT scans for lung tumors in the upper and middle lobe.[15] They concluded that the addition of a symmetrical 3D margin of 5 mm to a single slow CT ensured coverage of the "optimal" target volume derived from summation of the target volumes from multiple slow CT scans when only a single slow CT scan was used for treatment planning. Our results are nearly in agreement with the conclusion in regard to the transaxial plane, except in the CC direction. Our CT slice thickness of 1.25 mm is thinner than in their study where the CT slice thickness was 4 mm.[15] Thin-slice CT improves longitudinal resolution and enhances tumor detectability in the CC direction. High longitudinal resolution can decrease partial volume effects and lead to accurate delineation in the CC direction. Thus, thinner CT slices would make it possible to reduce additional margins in the CC direction. Despite the difference in CT slice thickness between slow CT scan and 4D CT scan, the additional margins were smaller in the CC direction than in other directions. This indicates that our results might not be biased by these differences.

Since 1998 we have performed SBRT for more than 250 patients with lung tumor. Our target determination protocol in SBRT planning is traditionally based on the slow CT scan protocol, which includes x-ray fluoroscopic examination to help define the target volume.[7,23,33] Currently, 4D CT images are also utilized to confirm the target volume. We showed that $TV_{slow\ CT}$ was smaller than $TV_{4D\ CT}$ for most cases. When determining target volumes in clinical practice, however, lung tumor motion observed with x-ray fluoroscopy is considered. Therefore, the clinically determined target volume is usually larger than the $TV_{slow\ CT}$ of this study. In addition, both setup margin and the margin between the PTV and the field edge are 5 mm in the Japan Clinical Oncology Group (http://www.jcog.jp/) number 0403 protocol. Nagata *et al.* reported that our local control rate of SBRT was 97% for 48 Gy in four fractions with a median follow-up of 30 months,[7] which is comparable to other results.[3–6] Considering our clinical results, our traditional protocol of target determination might be clinically acceptable.

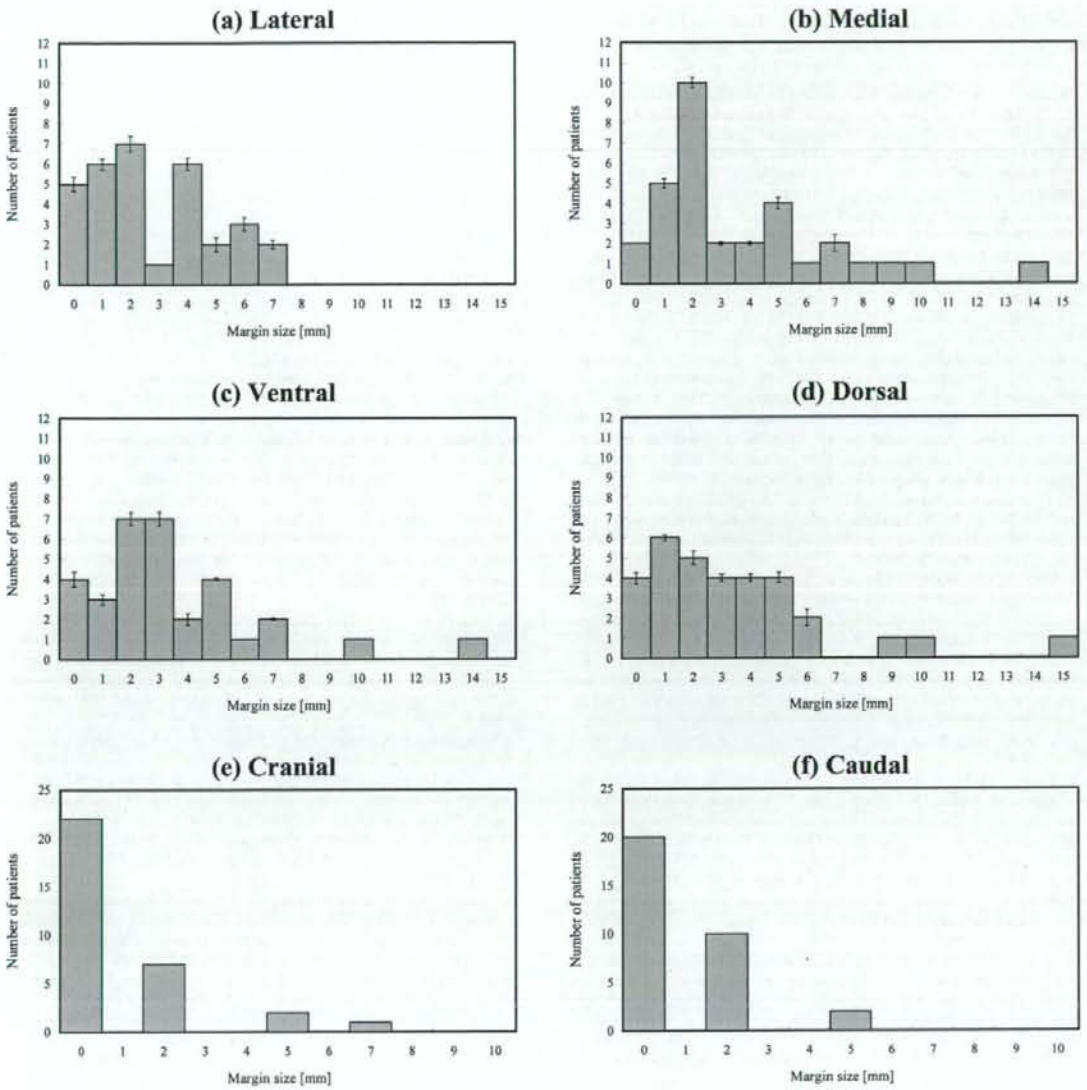

FIG. 4. Histograms of additional margins to the $TV_{slow\ CT}$ required for full coverage of $TV_{4D\ CT}$ for (a) lateral, (b) medial, (c) ventral, (d) dorsal, (e) cranial, and (f) caudal directions.

V. CONCLUSIONS

By comparing the target volume defined on slow CT images ($TV_{slow\ CT}$) with that defined on 4D CT images ($TV_{4D\ CT}$) for 32 lung tumors with motion range no larger than 8 mm in the upper and middle lobe, we evaluated geometrical differences between $TV_{slow\ CT}$ and $TV_{4D\ CT}$ and examined the additional margins needed for $TV_{slow\ CT}$ to ensure complete coverage of $TV_{4D\ CT}$. Our results revealed that a mean of 92% volume of $TV_{slow\ CT}$ was encompassed in $TV_{4D\ CT}$, and that additional margins to generate the target volume corresponding to $TV_{4D\ CT}$ are required even for lung tumors with motion range of 8 mm or less when only a single slow CT scan was used in treatment planning of SBRT.

ACKNOWLEDGMENTS

This study was conducted as part of the national project entitled "Fundamental investigation to develop a high-precision four-dimensional radiation therapy system," supported by the New Energy and Industrial Technology Development Organization (NEDO), and partly supported by a

Grant-in-Aid for Scientific Research from the Japan Society for the Promotion of Science (Grant No. 20229009).

[a]Author to whom correspondence should be addressed: Graduate School of Medicine, Kyoto University, Kyoto, 54 Kawara-cho, Shogoin, Sakyo-ku, Kyoto, 606-8507, Japan. Electronic mail: ynrt@kuhp.kyoto-u.ac.jp; Tel: (+81)-75-751-3762, Fax: (+81)-75-771-9749.

[1]F. J. Lagerwaard, S. Senan, J. P. van Meerbeeck, and W. J. Graveland, "Has 3-D conformal radiotherapy (3D CRT) improved the local tumour control for stage I non-small cell lung cancer?," Radiother. Oncol. **63**, 151–157 (2002).

[2]X. Qiao, O. Tullgren, I. Lax, F. Sirzén, and R. Lewensohn, "The role of radiotherapy in treatment of stage I non-small cell lung cancer," Lung Cancer **41**, 1–11 (2003).

[3]M. Uematsu, A. Shioda, A. Suda, T. Fukui, Y. Ozeki, Y. Hama, J. R. Wong, and S. Kusano, "Computed tomography-guided frameless stereotactic radiotherapy for stage I non-small cell lung cancer: A 5-year experience," Int. J. Radiat. Oncol., Biol., Phys. **51**, 666–670 (2001).

[4]R. Onimaru, H. Shirato, S. Shimizu, K. Kitamura, B. Xu, S. Fukumoto, T. C. Chang, K. Fujita, M. Oita, K. Miyasaka, M. Nishimura, and H. Dosaka-Akita, "Tolerance of organs at risk in small-volume, hypofractionated, image-guided radiotherapy for primary and metastatic lung cancers," Int. J. Radiat. Oncol., Biol., Phys. **56**, 126–135 (2003).

[5]R. Timmerman, L. Papiez, R. McGarry, L. Likes, C. DesRosiers, S. Frost, and M. Williams, "Extracranial stereotactic radioablation: results of a phase I study in medically inoperable stage I non-small cell lung cancer," Chest **124**, 1946–1955 (2003).

[6]J. Wulf, U. Haedinger, U. Oppitz, W. Thiele, G. Mueller, and M. Flentje, "Stereotactic radiotherapy for primary lung cancer and pulmonary metastases: A noninvasive treatment approach in medically inoperable patients," Int. J. Radiat. Oncol., Biol., Phys. **60**, 186–196 (2004).

[7]Y. Nagata, K. Takayama, Y. Matsuo, Y. Norihisa, T. Mizowaki, T. Sakamoto, M. Sakamoto, M. Mitsumori, K. Shibuya, N. Araki, S. Yano, and M. Hiraoka, "Clinical outcomes of a phase I/II study of 48 Gy of stereotactic body radiotherapy in 4 fractions for primary lung cancer using a stereotactic body frame," Int. J. Radiat. Oncol., Biol., Phys. **63**, 1427–1431 (2005).

[8]L. Potters, M. Steinberg, C. Rose, R. Timmerman, S. Ryu, J. M. Hevezi, J. Welsh, M. Mehta, D. A. Larson, and N. A. Janjan, "American Society for Therapeutic Radiology and Oncology and American College of Radiology practice guideline for the performance of stereotactic body radiation therapy," Int. J. Radiat. Oncol., Biol., Phys. **60**, 1026–1032 (2004).

[9]J. M. Balter, R. K. Ten Haken, T. S. Lawrence, K. L. Lam, and J. M. Robertson, "Uncertainties in CT-based radiation therapy treatment planning associated with patient breathing," Int. J. Radiat. Oncol., Biol., Phys. **36**, 167–174 (1996).

[10]S. Shimizu, H. Shirato, K. Kagei, T. Nishioka, X. Bo, H. Dosaka-Akita, S. Hashimoto, H. Aoyama, K. Tsuchiya, and K. Miyasaka, "Impact of respiratory movement on the computed tomographic images of small lung tumors in three-dimensional (3D) radiotherapy," Int. J. Radiat. Oncol., Biol., Phys. **46**, 1127–1133 (2000).

[11]G. T. Chen, J. H. Kung, and K. P. Beaudette, "Artifacts in computed tomography scanning of moving objects," Semin. Radiat. Oncol. **14**, 19–26 (2004).

[12]K. E. Rosenzweig, J. Hanley, D. Mah, G. Mageras, M. Hunt, S. Toner, C. Burman, C. C. Ling, B. Mychalczak, Z. Fuks, and S. A. Leibel, "The deep inspiration breath-hold technique in the treatment of inoperable non-small-cell lung cancer," Int. J. Radiat. Oncol., Biol., Phys. **48**, 81–87 (2000).

[13]D. Mah, J. Hanley, K. E. Rosenzweig, E. Yorke, L. Braban, C. C. Ling, S. A. Leibel, and G. Mageras, "Technical aspects of the deep inspiration breath-hold technique in the treatment of thoracic cancer," Int. J. Radiat. Oncol., Biol., Phys. **48**, 1175–1185 (2000).

[14]G. S. Mageras and E. Yorke, "Deep inspiration breath hold and respiratory gating strategies for reducing organ motion in radiation treatment," Semin. Radiat. Oncol. **14**, 65–75 (2004).

[15]F. J. Lagerwaard, J. R. van Sörnsen de Koste, M. R. Nijssen-Visser, R. H. Schuchhard-Schipper, S. S. Oei, A. Munne, and S. Senan, "Multiple "slow" CT scans for incorporating lung tumor mobility in radiotherapy planning," Int. J. Radiat. Oncol., Biol., Phys. **51**, 932–937 (2001).

[16]J. R. van Sörnsen de Koste, F. J. Lagerwaard, H. C. de Boer, M. R. Nijssen-Visser, and S. Senan, "Are multiple CT scans required for planning curative radiotherapy in lung tumors of the lower lobe?" Int. J. Radiat. Oncol., Biol., Phys. **55**, 1394–1399 (2003).

[17]J. R. van Sörnsen de Koste, F. J. Lagerwaard, M. R. Nijssen-Visser, W. J. Graveland, and S. Senan, "Tumor location cannot predict the mobility of lung tumors: a 3D analysis of data generated from multiple CT scans," Int. J. Radiat. Oncol., Biol., Phys. **56**, 348–354 (2003).

[18]E. C. Ford, G. S. Mageras, E. Yorke, and C. C. Ling, "Respiration-correlated spiral CT: a method of measuring respiratory-induced anatomic motion for radiation treatment planning," Med. Phys. **30**, 88–97 (2003).

[19]G. S. Mageras, A. Pevsner, E. D. Yorke, K. E. Rosenzweig, E. C. Ford, A. Hertanto, S. M. Larson, D. M. Lovelock, Y. E. Erdi, S. A. Nehmeh, J. L. Humm, and C. C. Ling, "Measurement of lung tumor motion using respiration-correlated CT," Int. J. Radiat. Oncol., Biol., Phys. **60**, 933–941 (2004).

[20]R. W. Underberg, F. J. Lagerwaard, J. P. Cuijpers, B. J. Slotman, J. R. van Sörnsen de Koste, and S. Senan, "Four-dimensional CT scans for treatment planning in stereotactic radiotherapy for stage I lung cancer," Int. J. Radiat. Oncol., Biol., Phys. **60**, 1283–1290 (2004).

[21]E. Rietzel, T. Pan, and G. T. Chen, "Four-dimensional computed tomography: Image formation and clinical protocol," Med. Phys. **32**, 874–889 (2005).

[22]E. Rietzel, A. K. Liu, K. P. Doppke, J. A. Wolfgang, A. B. Chen, G. T. Chen, and N. C. Choi, "Design of 4D treatment planning target volumes," Int. J. Radiat. Oncol., Biol., Phys. **66**, 287–295 (2006).

[23]Y. Negoro, Y. Nagata, T. Aoki, T. Mizowaki, N. Araki, K. Takayama, M. Kokubo, S. Yano, S. Koga, K. Sasai, Y. Shibamoto, and M. Hiraoka, "The effectiveness of an immobilization device in conformal radiotherapy for lung tumor: Reduction of respiratory tumor movement and evaluation of the daily setup accuracy," Int. J. Radiat. Oncol., Biol., Phys. **50**, 889–898 (2001).

[24]S. Seki, A. Takeda, T. Nagaoka, H. M. Deloar, T. Kawase, J. Fukuda, O. Kawaguchi, M. Uematsu, and A. Kubo, "Differences in the definition of internal target volumes using slow CT alone or in combination with thin-slice CT under breath-holding conditions during the planning of stereotactic radiotherapy for lung cancer," Radiother. Oncol. **85**, 443–449 (2007).

[25]J. D. Bradley, A. N. Nofal, I. M. El Naqa, W. Lu, J. Liu, J. Hubenschmidt, D. A. Low, R. E. Drzymala, and D. Khullar, "Comparison of helical, maximum intensity projection (MIP), and averaged intensity (AI) 4D CT imaging for steraotactic body radiation therapy (SBRT) planning in lung cancer," Radiother. Oncol. **81**, 264–268 (2006).

[26]B. Murray, K. Forster, and R. Timmerman, "Frame-based immobilization and targeting for stereotactic body radiation therapy," Med. Dosim. **32**, 86–91 (2007).

[27]S. Senan, J. van Sörnsen de Koste, M. Samson, H. Tankink, P. Jansen, P. J. Nowak, A. D. Krol, P. Schmitz, and F. J. Lagerwaard, "Evaluation of a target contouring protocol for 3D conformal radiotherapy in non-small cell lung cancer," Radiother. Oncol. **53**, 247–255 (1999).

[28]P. Bowden, R. Fisher, M. Mac Manus, A. Wirth, G. Duchesne, M. Millward, A. McKenzie, J. Andrews, and D. Ball, "Measurement of lung tumor volumes using three-dimensional computer planning software," Int. J. Radiat. Oncol., Biol., Phys. **53**, 566–573 (2002).

[29]Y. Matsuo, K. Takayama, Y. Nagata, E. Kunieda, K. Tateoka, N. Ishizuka, T. Mizowaki, Y. Norihisa, M. Sakamoto, Y. Narita, S. Ishikura, and M. Hiraoka, "Interinstitutional variations in planning for stereotactic body radiation therapy for lung cancer," Int. J. Radiat. Oncol., Biol., Phys. **68**, 416–425 (2007).

[30]Y. Seppenwoolde, H. Shirato, K. Kitamura, S. Shimizu, M. Van Herk, J. V. Lebesgue, and K. Miyasaka, "Precise and real-time measurement of 3D tumor motion in lung due to breathing and heartbeat, measured during radiotherapy," Int. J. Radiat. Oncol., Biol., Phys. **53**, 822–834 (2002).

[31]C. Plathow, S. Ley, C. Fink, M. Puderbach, W. Hosch, A. Schmähl, J. Debus, and H. U. Kauczor, "Analysis of intrathoracic tumor mobility during whole breathing cycle by dynamic MRI," Int. J. Radiat. Oncol., Biol., Phys. **59**, 952–959 (2004).

[32]Q. S. Chen, M. S. Weinhous, F. C. Deibel, J. P. Ciezki, and R. M. Macklis, "Fluoroscopic study of tumor motion due to breathing: Facilitating precise radiation therapy for lung cancer patients," Med. Phys. **28**, 1850–1856 (2001).

[33]K. Takayama, Y. Nagata, Y. Negoro, T. Mizowaki, T. Sakamoto, M. Sakamoto, T. Aoki, S. Yano, S. Koga, and M. Hiraoka, "Treatment planning of stereotactic radiotherapy for solitary lung tumor," Int. J. Radiat. Oncol., Biol., Phys. **61**, 1565–1571 (2005).

Int. J. Radiation Oncology Biol. Phys., Vol. 72, No. 2, pp. 398–403, 2008

0360-3016/08/$–see front matter

ELSEVIER

doi:10.1016/j.ijrobp.2008.01.002

CLINICAL INVESTIGATION **Lung**

STEREOTACTIC BODY RADIOTHERAPY FOR OLIGOMETASTATIC LUNG TUMORS

YOSHIKI NORIHISA, M.D.,* YASUSHI NAGATA, M.D., PH.D.,* KENJI TAKAYAMA, M.D.,* YUKINORI MATSUO, M.D., PH.D.,* TAKASHI SAKAMOTO, M.D.,† MASATO SAKAMOTO, M.D.,‡ TAKASHI MIZOWAKI, M.D., PH.D.,* SHINSUKE YANO, B.S.,* AND MASAHIRO HIRAOKA, M.D., PH.D.*

*Department of Radiation Oncology and Image-Applied Therapy, Kyoto University Graduate School of Medicine, Kyoto, Japan; †Department of Radiation Oncology, Kumamoto University Graduate School of Medical Sciences, Kumamoto, Japan; and ‡Department of Radiology, Japanese Red Cross Society Wakayama Medical Center, Wakayama, Japan

Purpose: Since 1998, we have treated primary and oligometastatic lung tumors with stereotactic body radiotherapy (SBRT). The term "oligometastasis" is used to indicate a small number of metastases limited to an organ. We evaluated our clinical experience of SBRT for oligometastatic lung tumors.

Methods and Materials: A total of 34 patients with oligometastatic lung tumors were included in this study. The primary involved organs were the lung (n = 15), colorectum (n = 9), head and neck (n = 5), kidney (n = 3), breast (n = 1), and bone (n = 1). Five to seven, noncoplanar, static 6-MV photon beams were used to deliver 48 Gy (n = 18) or 60 Gy (n = 16) at the isocenter, with 12 Gy/fraction within 4–18 days (median, 12 days).

Results: The overall survival rate, local relapse-free rate, and progression-free rate at 2 years was 84.3%, 90.0%, and 34.8%, respectively. No local progression was observed in tumors irradiated with 60 Gy. SBRT-related pulmonary toxicities were observed in 4 (12%) Grade 2 cases and 1 (3%) Grade 3 case. Patients with a longer disease-free interval had a greater overall survival rate.

Conclusion: The clinical result of SBRT for oligometastatic lung tumors in our institute was comparable to that after surgical metastasectomy; thus, SBRT could be an effective treatment of pulmonary oligometastases.

Stereotactic body radiotherapy, Metastatic lung tumor, Pulmonary metastases, Oligometastases.

INTRODUCTION

Stereotactic irradiation, stereotactic radiosurgery, and stereotactic radiotherapy are standard therapeutic techniques for intracranial tumors. With the introduction of three-dimensional localization techniques using a localizing frame of reference, hypofractionated irradiation using a stereotactic technique has been applied to extracranial tumors. Stereotactic body radiotherapy (SBRT) represents one of those treatments, and SBRT has been used in many institutes (1–9) mainly to irradiate lung or liver cancer.

Recently, patients with oligometastases, that is, a small number of metastatic lesions limited to an organ, have been considered candidates for curative treatment because long-term survival can be expected (10–13); therefore, surgical resection is the standard choice for patients with oligometastatic lung cancer. Since the effectiveness of SBRT for primary lung cancer was reported (5, 7, 14–17), awareness has been growing of SBRT as an effective option for curative treatment of lung tumors. In 1998, we began using SBRT for both primary and oligometastatic lung tumors. In this study, we retrospectively analyzed our experience with SBRT outcomes for oligometastatic lung tumors and reviewed the published data.

METHODS AND MATERIALS

Patient and tumor characteristics

The eligibility criteria of SBRT for oligometastatic lung tumor were as follows: *(1)* one or two pulmonary metastases, *(2)* tumor diameter ≤4 cm, *(3)* locally controlled primary tumor, and *(4)* no other metastatic sites. Of the patients treated between December 1998 and December 2004, 34 with oligometastatic lung tumors were included in this study. The primary involved organs were the lung (n = 15), colorectum (n = 9), head and neck (n = 5), kidney (n = 3), breast (n = 1), and bone (n = 1). Of these 34 patients, 25 were treated for

Reprint requests to: Yasushi Nagata, M.D., Ph.D., Department of Radiation Oncology and Image-Applied Therapy, Kyoto University Graduate School of Medicine, 54 Shogoin-Kawahara-Cho, Sakyo-Ku, Kyoto 606-8507, Japan. Tel: (+81) 75-751-3762; Fax: (+81) 75-751-3418; E-mail: nag@kuhp.kyoto-u.ac.jp

Supported by Grant-in-Aid H18-014 from the Ministry of Health, Labour and Welfare, Japan and Grant-in-Aid 18390333 from the Ministry of Education and Science, Japan.

Presented in part at the 46th Annual Meeting of the American Society for Therapeutic Radiology and Oncology (ASTRO), Atlanta, GA, October 3–7, 2004.

Conflict of interest: none.

Received Feb 5, 2007, and in revised form Dec 27, 2007. Accepted for publication Jan 3, 2008.

a single pulmonary nodule and 9 for two lesions. The histologic diagnosis of the primary disease was adenocarcinoma in 22, squamous cell carcinoma in 5, renal cell carcinoma in 3, adenoid cystic carcinoma in 2, pleomorphic carcinoma in 1, and osteosarcoma in 1 patient. Lung metastases were diagnosed clinically according to repeated thoracic computed tomography (CT) findings. Most patients had previously undergone surgical resection and chemotherapy for their primary cancer. Adjuvant oral chemotherapy regimens after SBRT were allowed. The patient characteristics are given in Table 1.

SBRT procedure

We used a combined X-ray and CT simulator—an integrated system using the same couch for the X-ray and CT simulators (Shimadzu, Kyoto, Japan). The patients were fixed in the stereotactic body frame (ELEKTA AB, Stockholm, Sweden) while CT scanning was performed with a slow scan time (4 s/slice).

Three-dimensional RT planning was performed using a treatment-planning machine (CADPLAN, version 3.1, and Eclipse, version 7.1, Varian Medical Systems, Palo Alto, CA). The internal target volume (ITV) was delineated on the CT images, considering the tumor motion assessed by X-ray fluoroscopy, and then the essential margins—planning target volume (PTV) margin and leaf margins—were added to the ITV (18, 19). We added 5 mm to the ITV for the PTV margin and another 5 mm from the contour of the PTV to the edge of the multileaf collimator for penumbra; thus, typically, a 10-mm margin was used between the contour of the ITV and the edge of the multileaf collimator. We used five to seven noncoplanar, static 6-MV photon beams and irradiated 12 Gy in each fraction at the isocenter. The patients received four or five fractions; therefore, the total dose was 48 Gy or 60 Gy at the isocenter within 4–18 days (median, 12 days).

Because we experienced several local failures with 48 Gy, the prescribed dose was escalated to 60 Gy from January 2001. However, the dose for metastases from primary lung cancer was maintained at 48 Gy because of difficulties in distinguishing a second primary lung cancer from a metastatic lesion and because the 5-year local relapse-free rate of 95% using this dose (16) was satisfactory. Also, the general pulmonary function was better in patients with metastatic lung cancer than in those with primary lung cancer. With the exception of patients with poor pulmonary function, a total dose of 60 Gy was prescribed to patients with a primary cancer other than lung cancer.

Table 1. Patient characteristics

Characteristic	Value
Patients (*n*)	34
Gender (*n*)	
Male	22
Female	12
Age (y)	
Range	30–80
Median	71
Performance status	
0	23
1	9
2	2
3–5	0
Primary tumor	
Lung	15
Colorectum	9
Head and neck	5
Kidney (renal cell carcinoma)	3
Bone (osteosarcoma)	1
Breast	1

Evaluation

The local response was assessed using the Response Evaluation Criteria in Solid Tumors and categorized into four types: *(1)* the disappearance of all target lesions (complete response), *(2)* at least a 30% decrease in the sum of the longest diameter of the target lesions (partial response), *(3)* a response ranging from a 30% decrease to a 20% increase in the sum of the longest diameter of the target lesions (stable disease), and *(4)* a ≥20% increase in the sum of the longest diameter of the target lesions (progressive disease). Because of the presence of consolidation with unclear margins around the tumor (20), it can be difficult to distinguish between tumor regrowth and radiation-induced injury; such cases were categorized as stable disease until apparent tumor regrowth was detected by careful and appropriate clinical observation for several months.

Survival was calculated from the first day of RT to the last day of follow-up. For overall survival, lost patients with clinically progressive disease and those with the terminal stage of disease were censored as dead. Adverse events were classified according to the Common Terminology Criteria for Adverse Events, version 3.

Statistical calculations were performed using Prism, version 4, software (GraphPad Software, San Diego, CA). The survival rates were analyzed using the Kaplan-Meier method, and differences in their distributions were evaluated using the log–rank test.

RESULTS

The study population comprised 22 men and 12 women, with median age of 71 years (range, 30–80 years). Of these 34 patients, 17 received 48 Gy in four fractions and 16 received 60 Gy in five fractions. One patient received 48 Gy in five fractions because of poor pulmonary function that necessitated a reduction in the fractional dose. The overall treatment time was 4–14 days (median, 12 days), except for

Table 2. Treatment results

Variable	Value
Tumor total (*n*)	43
Tumor diameter (*n*)	
<15 mm	17
≥15 but ≤30 mm	22
>30 mm	4
Prescribed dose (Gy)	
48	18
60	16
Overall treatment time (d)	
Range	4–18
Median	12
Follow-up period (mo)	
Range	10–80
Median	27

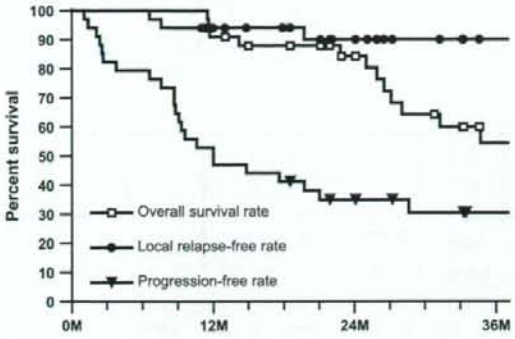

Fig. 1. Overall survival, local relapse-free survival, and progression-free survival rates after stereotactic body radiotherapy for oligometastatic lung cancer.

1 patient, for whom it was 18 days. The median follow-up period was 27 months (range, 10–80 months; Table 2).

Response

The overall survival rate, local relapse-free rate, and progression-free rate at 2 years was 84.3%, 90.0%, and 34.8%, respectively (Fig. 1). The numbers of patients with a complete response, partial response, stable disease, and progressive disease was 5, 8, 18, and 3, respectively. No statistically significant difference was found between those receiving 60 Gy and those receiving 48 Gy in terms of overall survival (p = 0.192; Fig. 2a); however, a marginally significant difference was observed between those receiving 60 Gy and 48 Gy in local progression-free survival (p = 0.078; Fig. 2b). No local progression was observed in tumors irradiated to 60 Gy, but three had local progression at 48 Gy. No differences were found in overall survival between patients with metastases from lung cancer and those with metastases from other cancers (p = 0.75).

Patterns of failure

Disease progression was observed in 23 patients (Table 3). Regrowth of the target lesions of SBRT was observed in 3 patients and recurrence of the primary lesion in 2. New metastatic lesions were observed in 19 patients. New intrapulmonary metastases were observed in 9 patients, and mediastinal or hilar regional lymph nodal metastases developed in 6. Distant metastases were observed in 3 patients: the adrenal gland in 2 and the liver in 1. One patient was diagnosed with progressive disease because of elevations of carcinoembryonic antigen and underwent chemotherapy.

Toxicity

The adverse events resulting from SBRT were classified using the Common Terminology Criteria for Adverse Events, version 3 (Table 4). Pulmonary toxicity was observed as cough, hemosputum, dyspnea, pleural effusion, and radiographic changes and was Grade 1 in 23 patients (68%) and Grade 2 in 4 (12%). One patient required oxygen

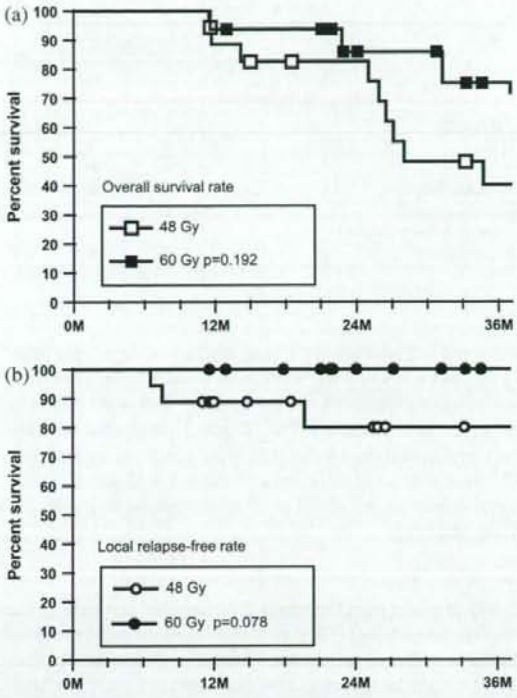

Fig. 2. (a) Overall survival rates of patients treated with 48 Gy and 60 Gy. (b) Local relapse-free rates of patients treated with 48 Gy and 60 Gy. Difference was marginally significant (p = 0.078).

supplementation for bacterial pneumonia 18 months after SBRT and was considered to have Grade 3 pulmonary toxicity. The symptoms of most patients were mild and did not interfere with their activities of daily living. Grade 1 skin toxicity with faint erythema or pigmentation with or without symptoms was observed in 6 patients (17%). One patient had a skin ulcer at the site of the reirradiated field, contralateral to the site of SBRT, and was cured with conservative treatment. Musculoskeletal adverse events were

Table 3. Patterns of disease progression

Pattern	*n*
New pulmonary metastasis	9
Regional lymph node metastasis	6
Local regrowth of target lesion of SBRT	3
Recurrence of primary lesion	2
Adrenal gland metastasis	2
Liver metastasis	1
Tumor marker elevation without any apparent recurrence	1

Abbreviation: SBRT = stereotactic body radiotherapy.

Of 34 patients, disease progression observed in 23 patients; 1 patient had regrowth at site of SBRT and liver metastasis simultaneously.

Table 4. Toxicity

Toxicity	Grade 0	1	2	3
Pulmonary	6	23	4	1
Skin	27	6	1	0
Pain	27	6	0	0
Musculoskeletal	32	2	0	0
Cardiac general (pericardial effusion)	32	2	0	0
Hepatobiliary	33	1	0	0

Total number of patients was 34.

observed in 2 patients (6%): bone fracture of the rib and musculitis of the chest wall. With these dermatologic or musculoskeletal complications of the thoracic wall, mild pain was observed in 6 patients (17%). Grade 1 pericardial effusion and temporal liver dysfunction were observed in 1 patient (3%) each. Most adverse events remained at Grade 1. No adverse effects of the spinal cord, great vessels, or esophagus were observed.

Prognostic factors

We also analyzed the survival differences stratified by the disease-free interval (DFI), previous chemotherapy, previous thoracic surgery, performance status, nodule size (sum of longer diameters), and number of targets. Except for DFI, no significant differences were observed. We stratified patients into three groups according to the DFI; <1 year, >1 year but <3 years, and >3 years (Fig. 3). Patients with DFI >3 years had significantly greater overall survival (p = 0.02) among the three groups. However, other factors showed negative results, which might suggest a limitation of this small group study.

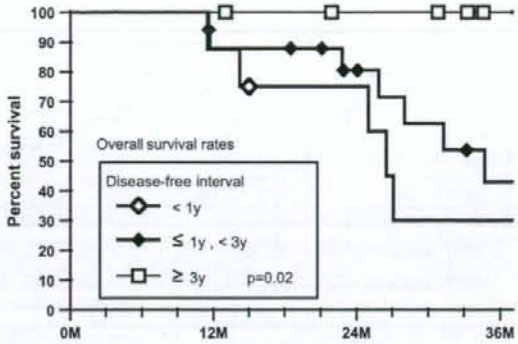

Fig. 3. Overall survival rates stratified by disease-free interval (p = 0.02).

DISCUSSION

Our clinical standard dose fractionation of SBRT for primary lung cancer was 48 Gy in four fractions. For metastatic lung cancer, we escalated the dose to 60 Gy because three local failures occurred with the 48-Gy dose. At last follow-up, 60 Gy appears to have been well tolerated by the patients with lung metastases. No local progression occurred with the 60-Gy dose. The difference between 48 and 60 Gy was not statistically significant in the survival rate, but was marginally significant (p = 0.078) in the local progression rate. The incidence of Grade 1 and 2 pulmonary toxicity was comparable between the two doses, with 13 (72%) and 2 (11%) at 48 Gy and 10 (63%) and 2 (13%) at 60 Gy, respectively. Dose escalation from 48 to 60 Gy increased the local control rate without increasing the incidence or severity of pulmonary toxicity.

Several reports have been published regarding the outcomes of SBRT for primary or metastatic lung tumors. Table 5 lists the survival outcomes after SBRT for pulmonary metastases in these reports. Onimaru *et al.* (8) and Wulf (14) reported overall survival rates of 49% and 33% at 2 years. Lee *et al.* (7) did not report the actuarial 2-year survival rate, although we calculated the crude survival rate to be 68% from data in their summary table. In the present study, it was 84%. The biologically effective dose, assuming the α/β ratio to be 10 (BED_{10}), in the present study was 105.6 Gy and 132.0 Gy for 48 Gy in four fractions and 60 Gy in five fractions, respectively. Onishi *et al.* (15) concluded that a BED_{10} of >100 Gy at the isocenter is preferable for the treatment of primary lung cancer to achieve a better overall survival rate. The BED_{10} of SBRT for pulmonary metastases ranged from 70 to 162 Gy, and the survival rates at 2 years ranged from 33% to 84% (Table 5).

An important aspect when discussing these results is the difference in treatment planning. One is the dose prescription point. We prescribed the dose to the isocenter. In contrast, some institutes prescribed to the margin of the PTV. Second is the PTV margin. The PTV margin differs depending on the setup accuracy at each institution. Third is the PTV contour. Contouring of the PTVs would reflect a difference in CT scanning: CT scanning with free breathing vs. breath holding and slow vs. fast scan times. Fourth is the dose calculation algorithm, including the inhomogeneity correction. Differences in the dose calculation algorithm would affect the marginal dose, particularly in treatment planning for lung tumors. Thus, we prescribed the dose to the isocenter to avoid unintended dose variations. Recently, more accurate dose calculation has become common, and adoption of a prescription with respect to the PTV is also worth considering, if a standard method has been established.

Surgical pulmonary metastasectomy has been recognized as a potentially curative treatment, particularly for patients without other metastases. Our published data review revealed that the 5-year survival rate for these patients was 26–40% (21–30) (Table 6). According to the International Registry of Lung Metastases, with >5,000 cases, surgical resection for metastatic lung tumor can result in long-term survival (21). In the International Registry of Lung

Table 5. SBRT for pulmonary metastases

Investigator	Primary tumor (*n*)	Patients (*n*)	Prescription	BED_{10} @ IC	Target	2-y Survival rate (%)
Lee *et al.* (7), 2003	Lung 5, liver 3, esophagus 2, trachea 2	19	30 Gy/3 Fr to 40 Gy/4 Fr		CTV: GTV + 5 mm	68*
		12	30 Gy/3 Fr (median 90% @ PTV margin)	70†	PTV: CTV + 5–10 mm	
		7	40 Gy/4 Fr (median 90% @ PTV margin)	94†		
Onimaru *et al.* (8), 2003	Lung 6, kidney 6, breast 2	20	48 Gy/8 Fr to 60 Gy/8 Fr		ITV	49
		15	48 Gy/8 Fr @ IC	76.8	PTV: ITV + 5–10 mm	
		5	60 Gy/8 Fr @ IC	105.0		
Wulf *et al.* (14), 2004	Lung 23, breast 5, colorectum 4, kidney 4, sarcoma 4	51	26 Gy/1 Fr to 37.5 Gy/3 Fr		CTV: GTV + 2–3 mm	33
		25	26 Gy/1 Fr (80% @ PTV margin)	138†	PTV: CTV+ 5–10 mm	
		12	30 Gy/3 Fr (100% @ PTV margin, 150% @ IC)	112.5		
		5	36 Gy/3 Fr (100% @ PTV margin, 150% @ IC)	151.2		
		9	37.5 Gy/3 Fr (100% @ PTV margin, 150% @ IC)	161.7		
Present study	Lung 15, colorectum 9, head and neck 5, kidney 3	34	48 Gy/4 Fr to 60 Gy/5 Fr		ITV	84
		18	48 Gy/4 Fr @ IC	105.6	PTV: ITV + 5 mm	
		16	60 Gy/5 Fr @ IC	132.0		

Abbreviations: SBRT = stereotactic body radiotherapy; BED_{10} = biologically effective dose ($\alpha/\beta = 10$); IC = isocenter; Fr = fractions; CTV = clinical target volume; GTV = gross tumor volume; PTV = planning target volume; ITV = internal target volume.

* Calculated from patient summary table.

† Estimations according to their marginal doses.

Metastases study, with the exclusion of the apparently favorable tumors (*i.e.*, germ cell and Wilms tumors), the survival outcome at 2 years was approximately 70%. In our study, the overall survival rate at 2 years was 84%. Thus, SBRT appears to have the potential to cure, similar to that of surgical metastasectomy.

Table 6. Results of metastasectomy

Investigator	Year	Primary cancer	Patients (n)	5-y Survival rate (%)
IRLM (21)	1997	Various	4,572	36
		Epithelial tumor	1,984	
		Sarcoma	1,917	
		Germ cell tumor	318	
		Melanoma	282	
		Other	70	
van Rens *et al.* (23)	2001	Lung	121	26
Saito *et al.* (25) (KCOG)	2002	Colorectum	165	40
Pfannschmidt *et al.* (27)	2003	Colorectum	167	32

Abbreviations: IRLM = International Registry of Lung Metastases; KCOG = Kansai Clinical Oncology Group.

The International Registry of Lung Metastases also analyzed prognostic factors. They found that a DFI of ≥36 months, a single metastasis, and germ cell or Wilms tumor as the primary tumor were factors resulting in a good prognosis. In our study, a longer DFI of >3 years was also a good prognostic factor. They also showed that the difference in relative risk was not substantial for those with common epithelial cancers such as those of the bowel, breast, head and neck, and kidney. In our study, no significant difference was found in overall survival between those with metastases from lung cancer and those with metastases from other sites. For selected patients with pulmonary oligometastases, survival after SBRT might not be affected by the primary disease.

CONCLUSION

The optimal regimen of SBRT for pulmonary metastasis has not yet been determined: 60 Gy was well tolerable and was superior to 48 Gy for local control at 2 years. SBRT for oligometastatic lung tumors was comparable to surgical metastasectomy with regard to the 2-year overall survival rate. SBRT could be an effective treatment for oligometastatic lung tumors.

REFERENCES

1. Uematsu M, Shioda A, Tahara K, *et al.* Focal, high dose, and fractionated modified stereotactic radiation therapy for lung carcinoma patients: A preliminary experience. *Cancer* 1998;82: 1062–1070.
2. Nakagawa K, Aoki Y, Tago M, *et al.* Megavoltage CT-assisted stereotactic radiosurgery for thoracic tumors: Original research in the treatment of thoracic neoplasms. *Int J Radiat Oncol Biol Phys* 2000;48:449–457.
3. Wulf J, Hadinger U, Oppitz U, *et al.* Stereotactic radiotherapy of extracranial targets: CT-simulation and accuracy of treatment in the stereotactic body frame. *Radiother Oncol* 2000;57:225–236.
4. Hara R, Itami J, Kondo T, *et al.* Stereotactic single high dose irradiation of lung tumors under respiratory gating. *Radiother Oncol* 2002;63:159–163.
5. Nagata Y, Negoro Y, Aoki T, *et al.* Clinical outcomes of 3D conformal hypofractionated single high-dose radiotherapy for one or two lung tumors using a stereotactic body frame. *Int J Radiat Oncol Biol Phys* 2002;52:1041–1046.
6. Hof H, Herfarth KK, Munter M, *et al.* Stereotactic single-dose radiotherapy of stage I non-small-cell lung cancer (NSCLC). *Int J Radiat Oncol Biol Phys* 2003;56:335–341.
7. Lee SW, Choi EK, Park HJ, *et al.* Stereotactic body frame based fractionated radiosurgery on consecutive days for primary or metastatic tumors in the lung. *Lung Cancer* 2003;40:309–315.
8. Onimaru R, Shirato H, Shimizu S, *et al.* Tolerance of organs at risk in small-volume, hypofractionated, image-guided radiotherapy for primary and metastatic lung cancers. *Int J Radiat Oncol Biol Phys* 2003;56:126–135.
9. Onishi H, Kuriyama K, Komiyama T, *et al.* A new irradiation system for lung cancer combining linear accelerator, computed tomography, patient self-breath-holding, and patient-directed beam-control without respiratory monitoring devices. *Int J Radiat Oncol Biol Phys* 2003;56:14–20.
10. Singh D, Yi WS, Brasacchio RA, *et al.* Is there a favorable subset of patients with prostate cancer who develop oligometastases? *Int J Radiat Oncol Biol Phys* 2004;58:3–10.
11. Kavanagh BD, McGarry RC, Timmerman RD. Extracranial radiosurgery (stereotactic body radiation therapy) for oligometastases. *Semin Radiat Oncol* 2006;16:77–84.
12. Yang JC, Abad J, Sherry R. Treatment of oligometastases after successful immunotherapy. *Semin Radiat Oncol* 2006;16: 131–135.
13. Rubin P, Brasacchio R, Katz A. Solitary metastases: Illusion versus reality. *Semin Radiat Oncol* 2006;16:120–130.
14. Wulf J, Haedinger U, Oppitz U, *et al.* Stereotactic radiotherapy for primary lung cancer and pulmonary metastases: A noninvasive treatment approach in medically inoperable patients. *Int J Radiat Oncol Biol Phys* 2004;60:186–196.
15. Onishi H, Araki T, Shirato H, *et al.* Stereotactic hypofractionated high-dose irradiation for stage I nonsmall cell lung carcinoma: Clinical outcomes in 245 subjects in a Japanese multiinstitutional study. *Cancer* 2004;101:1623–1631.
16. Nagata Y, Takayama K, Matsuo Y, *et al.* Clinical outcomes of a phase I/II study of 48 Gy of stereotactic body radiotherapy in 4 fractions for primary lung cancer using a stereotactic body frame. *Int J Radiat Oncol Biol Phys* 2005;63: 1427–1431.
17. Zimmermann FB, Geinitz H, Schill S, *et al.* Stereotactic hypofractionated radiation therapy for stage I non-small cell lung cancer. *Lung Cancer* 2005;48:107–114.
18. Negoro Y, Nagata Y, Aoki T, *et al.* The effectiveness of an immobilization device in conformal radiotherapy for lung tumor: Reduction of respiratory tumor movement and evaluation of the daily setup accuracy. *Int J Radiat Oncol Biol Phys* 2001; 50:889–898.
19. Takayama K, Nagata Y, Negoro Y, *et al.* Treatment planning of stereotactic radiotherapy for solitary lung tumor. *Int J Radiat Oncol Biol Phys* 2005;61:1565–1571.
20. Aoki T, Nagata Y, Negoro Y, *et al.* Evaluation of lung injury after three-dimensional conformal stereotactic radiation therapy for solitary lung tumors: CT appearance. *Radiology* 2004;230: 101–108.
21. The International Registry of Lung Metastases. Long-term results of lung metastasectomy: Prognostic analyses based on 5206 cases. *J Thorac Cardiovasc Surg* 1997;113:37–49.
22. Asaph JW, Keppel JF, Handy JR Jr., *et al.* Surgery for second lung cancers. *Chest* 2000;118:1621–1625.
23. van Rens MT, Zanen P, de la Riviere AB, *et al.* Survival after resection of metachronous non-small cell lung cancer in 127 patients. *Ann Thorac Surg* 2001;71:309–313.
24. Sakamoto T, Tsubota N, Iwanaga K, *et al.* Pulmonary resection for metastases from colorectal cancer. *Chest* 2001;119: 1069–1072.
25. Saito Y, Omiya H, Kohno K, *et al.* Pulmonary metastasectomy for 165 patients with colorectal carcinoma: A prognostic assessment. *J Thorac Cardiovasc Surg* 2002;124: 1007–1013.
26. Rena O, Casadio C, Viano F, *et al.* Pulmonary resection for metastases from colorectal cancer: factors influencing prognosis: Twenty-year experience. *Eur J Cardiothorac Surg* 2002; 21:906–912.
27. Pfannschmidt J, Muley T, Hoffmann H, *et al.* Prognostic factors and survival after complete resection of pulmonary metastases from colorectal carcinoma: experiences in 167 patients. *J Thorac Cardiovasc Surg* 2003;126:732–739.
28. Inoue M, Ohta M, Iuchi K, *et al.* Benefits of surgery for patients with pulmonary metastases from colorectal carcinoma. *Ann Thorac Surg* 2004;78:238–244.
29. Monteiro A, Arce N, Bernardo J, *et al.* Surgical resection of lung metastases from epithelial tumors. *Ann Thorac Surg* 2004;77:431–437.
30. Kondo H, Okumura T, Ohde Y, *et al.* Surgical treatment for metastatic malignancies—Pulmonary metastasis: Indications and outcomes. *Int J Clin Oncol* 2005;10:81–85.

ORIGINAL CONTRIBUTION

日放腫会誌 J Jpn Soc Ther Radiol Oncol 20: 119-125, 2008

非侵襲的呼吸同期照射に向けた腹壁運動と肺腫瘍運動との相関解析

中村 光宏[*1]，成田 雄一郎[*1]，松尾 幸憲[*1]，植林 正流[*1]，中田 学[*2]，
矢野 慎輔[*2]，澤田 晃[*1]，溝脇 尚志[*1]，永田 靖[*3]，平岡 眞寛[*1]

CORRELATIVE ANALYSIS OF ABDOMINAL MOTION WITH LUNG TUMOR MOTION FOR NON-INVASIVE RESPIRATORY GATED RADIOTHERAPY

Mitsuhiro NAKAMURA[*1], Yuichiro NARITA[*1], Yukinori MATSUO[*1],
Masaru NARABAYASHI[*1], Manabu NAKATA[*2], Shinsuke YANO[*2], Akira SAWADA[*1],
Takashi MIZOWAKI[*1], Yasushi NAGATA[*3], Masahiro HIRAOKA[*1]

(Received 17 April 2008, accepted 4 August 2008)

Abstract: Purpose: The purposes of this study were to assess the correlation between lung tumor motion and the abdominal motion, and to estimate the position mismatch as the difference between the abdominal motion trace used to the predicted lung tumor position and the measured lung tumor position.
Methods and Materials: Eleven patients who underwent stereotactic body radiotherapy between December 2006 and March 2008 were included in this study. Of all the patients, 6 were studied over 3 days under an internal review board approved protocol. Breathing synchronized fluoroscopy was performed under free breathing. Measurements of the anterior-posterior abdominal skin surface displacement by the Real-time Positioning Management System (Varian Medical Systems, Inc., Palo Alto, CA) were correlated to simultaneously acquired X-ray fluoroscopy (Acuity; Varian Medical Systems, Inc.) measurements of superior-inferior tumor displacement. The lung tumor motion was analytically detected by a template matching algorithm after image processing. To evaluate the tumor-abdominal motion phase relationship, a cross-correlation was calculated of the time-synchronized tumor motion and the abdominal motion. By comparing the predicted lung tumor position in which phase difference was corrected to the measured lung tumor position, the position mismatch was computed.
Results: The correlation coefficients between the lung tumor motion and abdominal motion ranged 0.89 from 0.97 and more reproducible from day to day. A hysteresis curve was observed due to phase difference between the lung tumor motion and abdominal motion. The average of the position mismatch was up to 1.78 mm.
Conclusion: Even if the correlation coefficients between the abdominal motion and the tumor motion were high for most cases, there were some differences between the predicted lung tumor position and the measured lung tumor position.

Key words: Respiratory gated radiotherapy, Lung tumor motion, Respiration surrogate

はじめに

放射線治療における照射技術の高度化に伴い，体内臓器の呼吸性移動に対する関心がますます高まりつつある中，American Association of Physicists in Medicineは，呼吸性移動への対応に関する報告書を発表した[1]．これによると，X線透視や四次元CT，シネMRIなどで，腫瘍の呼吸性移動を評価した結果，場所によっては30mmに及ぶと報告されている．

呼吸性移動を伴う腫瘍に対して放射線治療を行う場合，腫瘍の移動範囲をすべて含んだ内的標的体積を設定し，更にセットアップマージンを加味した計画標的体積(以下，PTV)に対して照射野を設定する照射法(以下，motion inclusive法)が一般的である．呼吸性移動が小さい場合はmotion inclusive法でも，正常組織に対する線量を低く抑えつつ，PTVへの線量を確保することが可能であるが，呼吸性移動が大きい腫瘍に対してmotion inclusive法を適応すると，PTVサイズが結果的に大きくなり，正常組織に対する不必要な線量が多くなる．われわれは肺定位放射線治療において，腫瘍の呼吸性移動が大きい症例に対して，呼吸性移動抑制を目的とした腹部圧迫板を使用しているが，抑制効果が小さい場合や呼吸機能が悪いことが原因で腹部圧迫板を使用できない症例を経験している．

腫瘍に対する線量を確保しつつ，正常組織に対する線量を低減させる照射方法の一つとして，呼吸同期照射法がある．呼吸同期照射法は腫瘍に対して呼吸周期中の特定の位

[*1]京都大学大学院医学研究科放射線腫瘍学・画像応用治療学(〒606-8507 京都市左京区聖護院川原町54)(Department of Radiation Oncology and Image-applied Therapy, Kyoto University Graduate School of Medicine)(54 Shogoin-Kawaharacho, Sakyo-ku, Kyoto 606-8507, JAPAN)，[*2]京都大学医学部附属病院放射線部(Clinical Radiology Service, Kyoto University Hospital)，[*3]広島大学病院放射線治療部(Division of Radiation Oncology, Hiroshima University Hospital)

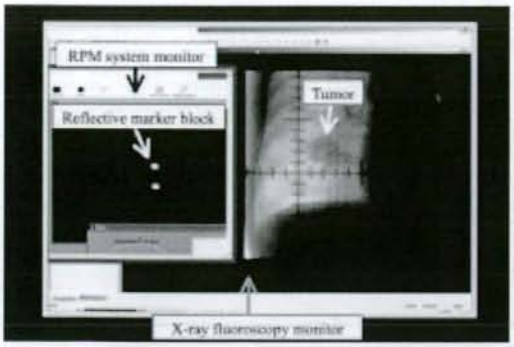

Fig. 1 A parallel display between RPM system monitor representing abdominal wall motion using a reflective marker block, and a chest fluoroscopic image from the anterior of a patient.

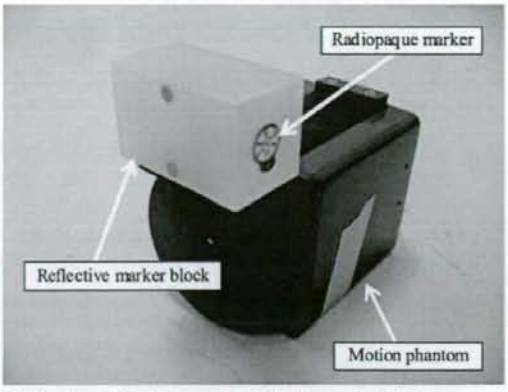

Fig. 2 A motion phantom and a reflective marker block.

相もしくは位置にタイミングを合わせて照射を行う方法であり，1980年代後半に日本で開始されて以来[2]，現在では多くの施設で施行されている[1]．この照射方法は，腫瘍近傍に留置された放射線不透過マーカー等を直接観測しながら照射を行う侵襲的呼吸同期照射と，腫瘍の呼吸性移動の代替信号として腹壁変位量や換気流量等を用いる非侵襲的呼吸同期照射に大別される[1]．

代替信号と体内臓器もしくは放射線不透過マーカーの相関性に関しては，多くの報告がなされている[3)-7)]．Mageras[3]やVedamら[4]は，腹壁変位量と横隔膜の頭尾方向の変位量の間に良好な位相の相関関係があると報告した．肺腫瘍に対して非侵襲的呼吸同期照射を実施する場合，横隔膜ではなく，肺腫瘍を直接評価する方が望ましいと考える．Ahn[5]やHoisakら[6]は，腹壁変位量もしくは換気流量と肺腫瘍の頭尾方向の変位量(以下，肺腫瘍変位量)を計測し，これらの間に大きな位相ずれが生じる場合があると報告した．高精度に非侵襲的呼吸同期照射を行うためには，代替信号が予測する腫瘍位置と実際の腫瘍位置との間に生じるずれ量(以下，腫瘍位置ずれ量)を考慮する必要があると考える．Ionascuら[7]は腫瘍近傍に留置された放射線不透過マーカー位置と腹壁変位量が予測した肺腫瘍位置のずれは頭尾方向で2.5mm以上に及ぶ場合があると報告したが，放射線不透過マーカーを使用せずに，腫瘍位置ずれ量を測定した報告はなされていない．

当院では呼吸性移動を伴う腫瘍に対して，腹壁変位量に基づく非侵襲的呼吸同期照射の臨床適用を検討している．本研究の目的は放射線不透過マーカーを使用せずに，X線シミュレーターで計測した肺腫瘍変位量と商用の呼吸同期照射システムで取得した腹壁変位量との位相相関性を評価し，腫瘍位置ずれ量を算出することである．

方　法

1. 使用機器

肺腫瘍変位量の観測にはX線シミュレーター(Acuity; Varian Medical Systems, Inc., Palo Alto, CA)を使用し，肺腫瘍変位量の代替信号である腹壁変位量の取得にはReal-time Positioning Managementシステム(以下，RPMシステム; Varian Medical Systems, Inc.)を使用した．RPMシステムでは，対象に貼付した赤外線反射マーカーからの反射赤外線をCCDカメラが受光し，30 frame/secで赤外線反射マーカー位置を検出した．

2. 画像収集及び解析方法

RPMシステム画面とX線透視画面の時間軸を一致させるために，Local Area Network(以下，LAN)を介したWindows XPのリモートデスクトップ機能を利用し，RPMシステム画面とX線透視画面を並列に表示した(Fig. 1)．LANのデータ転送速度の理論最大値は1Gbpsであり，また，X線シミュレーターとRPMシステムのみのネットワーク構成とすることで，信号遅延を抑制した．X線シミュレーターに接続したDVDドライブで，並列表示したRPMシステム画面とX線透視画面をDVDメディアに録画した．次に，DVDメディアに保存した時系列画像に対して，最大吸気位相，最大呼気位相及び中間位相における肺腫瘍テンプレートを用いたテンプレートマッチングにより，肺腫瘍位置を検出し，その頭尾方向の変位量を解析した．

1)信号遅延検証

LANを介したリモートデスクトップ機能の利用による信号遅延を検証した．RPMシステム付属の動体ファントムに設置した赤外線反射マーカー上に放射線不透過マーカーを貼付し，上下運動させた(Fig. 2)．X線シミュレーターのガントリーを90度回転させた状態で，約60秒間撮影(画像取得間隔：0.03秒，取得静止画像枚数：約1,800枚)し，リモートデスクトップ機能を利用して，RPMシステム画面とX線透視画面の並列表示画像を取得した．取得画像から二値化処理により，赤外線反射マーカー位置と放射線不透過マーカー位置を検出し，これらの相関係数を算出した．

Table 1 Individual patient characteristics

Patient	Age	Sex	Location	Multiple days
1	78	M	RLL	Yes
2	58	M	RML	No
3	77	M	RLL	Yes
4	62	F	LLL	Yes
5	81	M	LLL	No
6	81	M	LUL	Yes
7	77	F	RLL	Yes
8	78	M	RLL	No
9	78	M	RML	Yes
10	80	M	LLL	No
11	74	F	RLL	No

Abbreviations: M, male; F, female; RLL, right lower lobe; RML, right middle lobe; LLL, left lower lobe; LUL, left upper lobe.

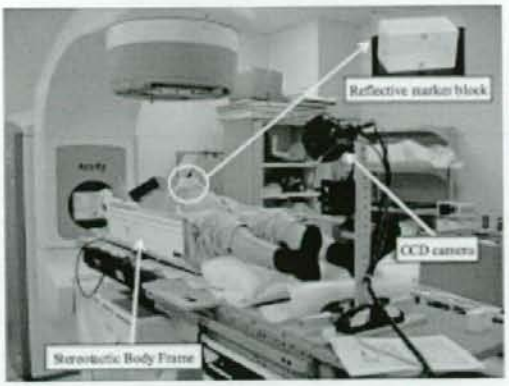

Fig. 3 Typical patient setup. A reflective marker block placed midway between the patient's xiphoid process and umbilicus was used in the recording of the respiration signal.

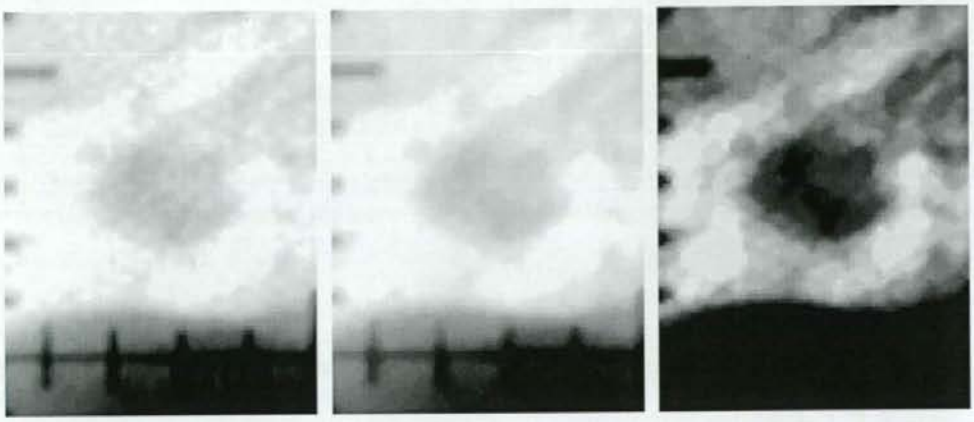

Fig. 4 An example of image processing.
(a) An original image.
(b) The median filter was used to reduce noise in images.
(c) The contrast between tumor and background was enhanced.

a | b | c

2)臨床画像

対象症例

2006年12月から2008年 3 月までの間に，当院で肺定位放射線治療を施行した症例のうち，X線透視画像上で肺腫瘍の同定が可能であり，その変位量が頭尾方向に平均で 8mm 以上と，複数の放射線腫瘍医によって判断された11症例を対象とした(Table 1)．

治療計画時に患者の固定具(stereotactic body frame; Elekta Corp., Stockholm, Sweden)を作成後，赤外線反射マーカーを患者の剣状突起と臍部の中心付近に貼付した(Fig. 3)．次に，X線シミュレーターのガントリー角度を 0 度とし，自由呼吸下で約60秒間撮影(画像取得間隔：0.03秒，取得静止画像枚数：約1,800枚)し，リモートデスクトップ機能を利用して，RPMシステム画面とX線透視画面の並列表示画像を取得した．尚，対象症例のうち 6 症例は倫理審査委員会の承認の下，治療期間中の 2 日間においても測定を行った．1回目測定(以下，Session 1)から 2 回目測定(以下，Session 2)までは少なくとも 5 日間以上開いており，3 回目測定(以下，Session 3)までの期間は最大で10日間であった．

画像処理及び解析

RPMシステム画像を二値化処理し，赤外線反射マーカー位置を検出した．次に，X線透視画像に対してカーネルサイズが 3×3 のメディアンフィルターを適用し，平滑化した．更に，肺腫瘍検出範囲内のピクセル値ヒストグラムの平坦化を行い，肺腫瘍とバックグラウンドのコントラストを強調した(Fig. 4)．肺腫瘍の動体追跡にはテンプレートマッ

Table 2 Tumor-abdominal motion correlation coefficients over all measurement sessions

Patient	Session 1	Session 2	Session 3
1	0.97	0.97	0.97
2	0.89	n/a	n/a
3	0.96	0.96	0.95
4	0.97	0.96	0.94
5	0.96	n/a	n/a
6	0.93	0.95	0.94
7	0.89	0.96	0.93
8	0.96	n/a	n/a
9	0.93	0.97	0.97
10	0.96	n/a	n/a
11	0.89	n/a	n/a

Abbreviation: n/a, not available (patient did not participate in this measurement session).

Table 3 Phase difference between superior-inferior tumor motion and anterior-posterior abdominal motion

Patient	Session 1	Session 2	Session 3
1	0.03	0.03	0.00
2	0.33	n/a	n/a
3	0.10	0.13	0.10
4	0.10	0.13	0.07
5	0.13	n/a	n/a
6	0.07	0.07	0.07
7	0.13	0.10	0.13
8	0.00	n/a	n/a
9	0.03	0.10	0.10
10	0.00	n/a	n/a
11	0.23	n/a	n/a

Abbreviation: n/a, not available (patient did not participate in this measurement session).
Notes: A positive value indicates that the lung tumor motion is lagging behind abdominal motion. All values are in seconds.

チングを使用した．肺腫瘍の呼吸性移動や変形及び骨構造との重なりによる誤検出を抑えるため，テンプレートには呼吸周期が安定している最大吸気位相，最大呼気位相，及び，その中間呼吸位相における 3 種類の画像を用意した．これにより，X線透視画像中の任意の呼吸位相における肺腫瘍検出能が向上するように工夫した．各テンプレート画像とX線透視画像の非類似度 $\left(D_k,\ k\in\{end\text{-}in,\ end\text{-}ex,\ mid\}\right)$ を式(1)～(3)で評価し，算出した非類似度が最小となる位置 (x^*, y^*) を肺腫瘍位置とした(式(4))．

$$D_{end\text{-}in}(x,y)=\sum_{i=0}^{M-1}\sum_{j=0}^{N-1}\left\{f(x+i,y+j)-g_{end\text{-}in}(i,j)\right\}^2 \quad (1)$$

$$D_{end\text{-}ex}(x,y)=\sum_{i=0}^{M-1}\sum_{j=0}^{N-1}\left\{f(x+i,y+j)-g_{end\text{-}ex}(i,j)\right\}^2 \quad (2)$$

$$D_{mid}(x,y)=\sum_{i=0}^{M-1}\sum_{j=0}^{N-1}\left\{f(x+i,y+j)-g_{mid}(i,j)\right\}^2 \quad (3)$$

$$(x^*,y^*)=\arg\min_{(x,y)\in R}\left(D_{end\text{-}in}(x,y),D_{end\text{-}ex}(x,y),D_{mid}(x,y)\right) \quad (4)$$

ここで，MとNはそれぞれテンプレート画像の縦と横のピクセル数，$f(x, y)$〔ただし，$(x, y)\in R$であり，肺腫瘍検出範囲内をRとした〕は，X線透視画像のピクセル位置(x, y)におけるピクセル値，$g_{end\text{-}in}(i,j)$，$g_{end\text{-}ex}(i,j)$ 及び $g_{mid}(i,j)$は，それぞれ最大吸気位相，最大呼気位相及び中間位相のテンプレート画像のピクセル値を表す．

肺腫瘍位置の検出後，腹壁変位量と肺腫瘍変位量の位相に対する相関係数及び位相ずれを算出した．得られた相関の有意性を検定するために，無相関検定を行った．また，相関係数が最も 1 に近づくように位相ずれを補正し，そこで得られた回帰直線を基に腹壁変位量が予測する肺腫瘍位置を求め，測定した肺腫瘍位置と比較することで，腫瘍位置ずれ量の平均値及び99%信頼区間を算出した．

結　果

1. 信号遅延検証

赤外線反射マーカー位置と放射線不透過マーカー位置の位相相関係数はほぼ 1 となり，LANを介したリモートデスクトップ機能を利用することによる信号遅延は無視できるほど小さかった．

2. 位相相関性

臨床画像における位相相関性及び位相ずれの解析結果を，それぞれTable 2 及びTable 3 に示す．複数日間にわたって測定を行った症例の日々の変動(以下，日間変動)は比較的安定していた(Table 2, Session 1-3)．相関係数の無相関検定を行った結果，すべてのSessionで$p<0.0001$であった．

呼吸パターンは必ずしも規則正しくはなく，測定中に呼吸パターンが不規則な症例も見られた．それらの中で，特徴的な相関図及び腹壁変位量と肺腫瘍変位量の時系列グラフをFig. 5, Fig. 6 及びFig. 7 に示す．患者 1 のSession 2 における時系列グラフでは，測定開始直後から15秒後まで，患者の呼吸が呼気位相で中断しており(Fig. 5a)，相関図中の呼気位相に集合体が形成された(Fig. 5b)．60秒間の測定においても，呼吸パターンは不規則であったが，相関係数の絶対値は0.97であった．患者 2 のSession 1 における時系列グラフでは，肺腫瘍変位量と腹壁変位量の間に位相ずれが観測された(Fig. 6a)．相関係数の絶対値は0.89であったが，その相関図はヒステリシス曲線を描いていた(Fig. 6b)．この場合，腫瘍位置ずれは顕著であった．患者 9 のSession 2 における時系列グラフでは，測定開始30秒後に深呼吸をしていた(Fig. 7a)．このとき，相関図中の軌跡は大きくはずれ，ループを描いていた(Fig. 7b)が，測定時間内における相関係数の絶対値は0.97であった．

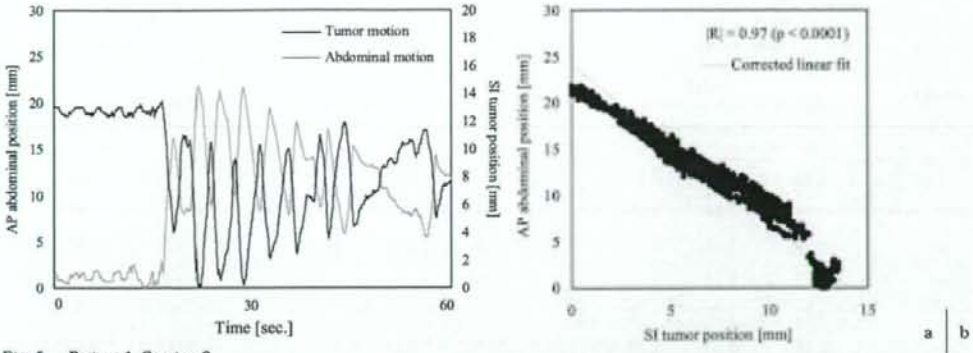

Fig. 5 Patient 1, Session 2
(a) Superior-inferior tumor motion and anterior-posterior abdominal motion as a function of time.
(b) Superior-inferior tumor position as a function of anterior-posterior abdominal position. Even if the respiratory pattern is irregular, the correlation coefficient is high ($|R|$=0.97; $p<0.0001$).

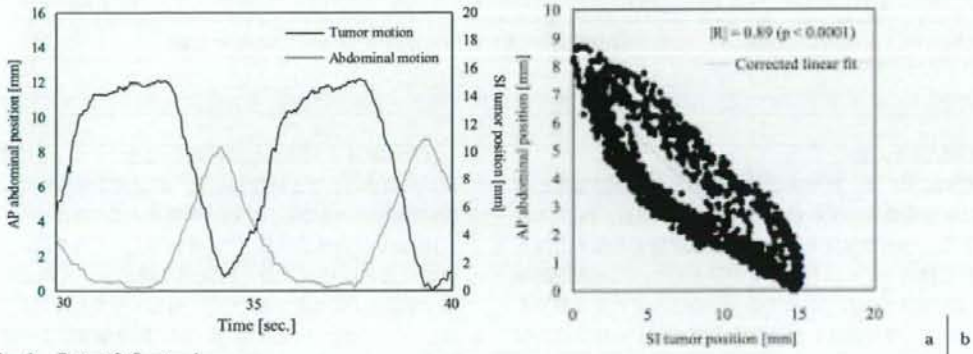

Fig. 6 Patient 2, Session 1
(a) Superior-inferior tumor motion and anterior-posterior abdominal motion as a function of time.
(b) Superior-inferior tumor position as a function of anterior-posterior abdominal position. The loop caused by respiratory phase lag between abdominal and tumor motion was observed ($|R|$=0.89; $p<0.0001$).

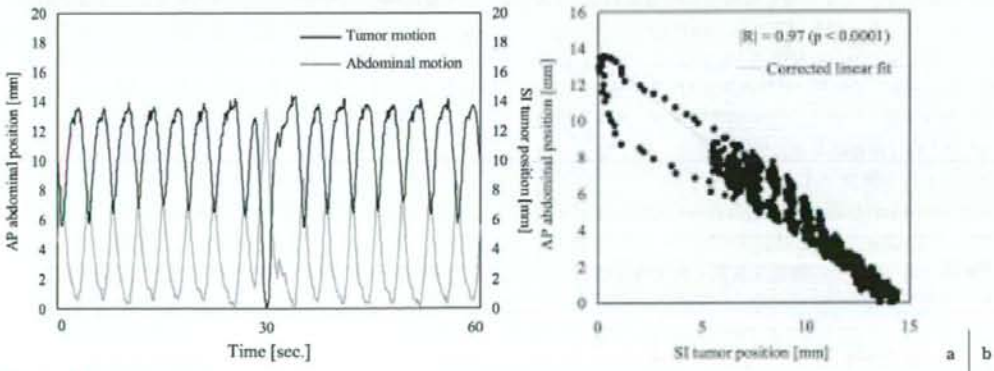

Fig. 7 Patient 9, Session 2
(a) Superior-inferior tumor motion and anterior-posterior abdominal motion as a function of time.
(b) Superior-inferior tumor position as a function of anterior-posterior abdominal position. The patient breathed deeply after 30 sec ($|R|$=0.97; $p<0.0001$).

Table 4 The position mismatch between the predicted tumor position and the measured tumor position

Patient	Session 1			Session 2			Session 3		
	Mean	99% C.I.		Mean	99% C.I.		Mean	99% C.I.	
		Lower	Upper		Lower	Upper		Lower	Upper
1	0.49	0.47	0.52	0.71	0.68	0.73	0.61	0.59	0.64
2	1.78	1.71	1.85		n/a			n/a	
3	1.70	1.63	1.77	0.88	0.85	0.92	1.00	0.95	1.06
4	1.21	1.15	1.26	1.26	1.18	1.33	0.61	0.58	0.64
5	1.42	1.35	1.49		n/a			n/a	
6	0.44	0.42	0.46	0.73	0.70	0.76	0.67	0.64	0.70
7	0.84	0.80	0.88	0.53	0.50	0.55	0.86	0.83	0.90
8	0.46	0.44	0.48		n/a			n/a	
9	0.77	0.73	0.81	0.45	0.42	0.48	0.69	0.66	0.71
10	1.73	1.66	1.81		n/a			n/a	
11	1.55	1.46	1.64		n/a			n/a	

Abbreviations: C.I., confidence interval; n/a, not available (patient did not participate in this measurement session).
Notes: All values are in millimeters.

3. 腫瘍位置ずれ量

全症例において，腹壁変位量が予測した肺腫瘍位置と測定した肺腫瘍位置にずれが認められた(Table 4)．Table 4 の平均値及び99%信頼区間幅から，腫瘍位置ずれ量の日内及び日間変動は一定ではないことが示された．同一患者間の位相相関係数が同じであっても，腫瘍位置ずれ量は異なる値を示した．深呼吸をした場合，腫瘍位置ずれ量は最大で5mmに及ぶことがわかった(Fig. 7b)．

考 察

本研究では，LANを介したリモートデスクトップ機能を利用し，RPMシステムで取得した腹壁変位量とX線シミュレーターから取得した肺腫瘍変位量の時間軸を同期させて解析することを試みた．信号遅延検証結果及び画像取得間隔が0.03秒であることから，信号遅延は0.03秒未満であり，赤外線反射マーカー位置及び放射線不透過マーカー位置の時系列データの時間軸は非常に高い精度で一致していた．

複数日にわたる測定では，患者のセットアップ，赤外線反射マーカーの貼付位置，皮膚のたるみや胃内の充満度の違い等で，CCDカメラと赤外線反射マーカーの幾何学的位置関係が異なる．しかし，腹壁変位量と肺腫瘍変位量の位相相関の日間変動が小さいことから，実臨床で想定される赤外線反射マーカーとCCDカメラの幾何学的位置関係の違いによる位相の相関性への影響は非常に小さいと考えられる．Ahnら[5]は，体表面に直接貼付した放射線不透過マーカーと腫瘍もしくは横隔膜との位相相関性を解析した結果，相関係数の平均値±標準偏差は0.77±0.12であり，特に下肺野の腫瘍や横隔膜と放射線不透過マーカーとの間には強い相関があったと結論付けた．本研究で得られた位相相関係数は0.95±0.03と，Ahnら[5]の結果よりも高かった．

Hoisakら[6]は独自のシステムを構築し，これを用いて肺腫瘍変位量と腹壁変位量との位相相関について検証した結果，相関係数は0.39から0.98と，幅広く分布していることを示した．位相相関が悪い症例では，肺腫瘍変位量と腹壁変位量で最大0.65秒の位相ずれが生じており，その相関図は位相ずれに起因するヒステリシス曲線を描いていた．本研究でも，例えば患者 2 のSession 1 における位相相関係数は高い値を示していたが，肺腫瘍変位量と腹壁変位量の間に0.33秒の位相ずれが生じていた(Fig. 6b)．位相ずれが発生する原因の一つとして，呼吸方式の差異が考えられる．呼吸方式には，横隔膜や腹筋を使う腹式呼吸と肋間筋を使う胸式呼吸の二種類がある．胸式呼吸では，吸気時において胸郭が広がると共に肺腫瘍が動き出し，続いて腹壁が動くため，腹壁変位量と肺腫瘍変位量の位相ずれが生じると考えられる．一方，腹式呼吸では，横隔膜及び腹壁が動き出すと同時に肺に空気が取り込まれ，それに伴って肺腫瘍も動き出すため，腹壁変位量と肺腫瘍変位量の相関は良好であると推測する．腹壁変位量を肺腫瘍変位量の代替信号として用いる場合，腹式呼吸へ誘導できれば，腹壁変位量と肺腫瘍変位量の相関が向上し，非侵襲的呼吸同期照射の高精度化が図れると考える．また，呼吸パターンが不規則な患者に対して呼吸コーチングを適用することにより，呼吸パターンの再現性が向上するだけでなく[3), 8)-11)]，呼吸同期照射の効率が向上すると報告されており[10), 11)]，非侵襲的呼吸同期照射のスループット向上との相乗効果も期待できる．

代替信号が正確に腫瘍の呼吸性移動を表現していない状態で非侵襲的呼吸同期照射を行うと，腫瘍に対して過小線量のまま治療が完遂する恐れがある．本研究では放射線不透過マーカーを使わずに腫瘍位置ずれ量が求まることを実証し，Ionascuら[7]と同様の結果を得た．位相に対して高い相関係数を示しても，腹壁変位量が予測した肺腫瘍位置と測定した肺腫瘍位置にはずれが生じており，この値を無視できない症例も見られた．これらのずれ量を実臨床に反映させるには，腫瘍位置ずれ量を保証するマージンの設定もしくは呼吸同期幅の拡大等の対応が必要と考える．ただし，今回得られた腫瘍位置ずれ量は60秒の測定時間から得られた値であり，1回当たりの治療時間が60秒よりも長い場合や腹壁変位量のベースラインシフト等の影響で，腫瘍位置ずれ量が更に大きくなる可能性も考えられる．

結　論

赤外線反射マーカーと肺腫瘍の動きを同時に計測及び解析できる方法を考案し，これらの位相相関性及び腹壁変位量が予測した肺腫瘍位置と測定した肺腫瘍位置のずれ量を解析した．多くの症例で，腹壁変位量と肺腫瘍変位量との位相の相関関係は良好であり，これらの日間変動も安定していた．しかし，腹壁変位量が予測した肺腫瘍位置と測定した肺腫瘍位置の間にずれが生じていた．

謝辞：本研究の遂行にあたり，ご協力を賜りました京都大学医学部附属病院放射線治療部門の皆様に，誌面を借りて深謝申し上げます．

本研究の一部は，平成20年度科学研究費補助金基盤研究(S)(課題番号：20229009)の一部として実施された．

文　献

1) Keall PJ, Mageras GS, Balter JM, et al.: The management of respiratory motion in radiation oncology report of AAPM Task Group 76. *Med Phys* **33**: 3874-3900, 2006.
2) Ohara K, Okumura T, Akisada M, et al.: Irradiation synchronized with respiration gate. *Int J Radiat Oncol Biol Phys* **17**: 853-857, 1989.
3) Mageras GS, Yorke E, Rosenzweig K, et al.: Fluoroscopic evaluation of diaphragmatic motion reduction with a respiratory gated radiotherapy system. *J Appl Clin Med Phys* **2**: 191-200, 2001.
4) Vedam SS, Kini VR, Keall PJ, et al.: Quantifying the predictability of diaphragm motion during respiration with a noninvasive external marker. *Med Phys* **30**: 505-513, 2003.
5) Ahn S, Yi B, Suh Y, et al.: A feasibility study on the prediction of tumour location in the lung from skin motion. *Br J Radiol* **77**: 588-596, 2004.
6) Hoisak JD, Sixel KE, Tirona PC, et al.: Correlation of lung tumor motion with external surrogate indicators of respiration. *Int J Radiat Oncol Biol Phys* **60**: 1298-1306, 2004.
7) Ionascu D, Jiang SB, Nishioka S, et al.: Internal-external correlation investigations of respiratory induced motion of lung tumors. *Med Phys* **34**: 3893-3903, 2007.
8) Kini VR, Vedam SS, Keall PJ, et al.: Patient training in respiratory-gated radiotherapy. *Med Dosim* **28**: 7-11, 2003.
9) Kubo HD and Wang L: Introduction of audio gating to further reduce organ motion in breathing synchronized radiotherapy. *Med Phys* **29**: 345-350, 2002.
10) George R, Chung TD, Vedam SS, et al.: Audio-visual biofeedback for respiratory-gated radiotherapy: Impact of audio instruction and audio-visual biofeedback on respiratory-gated radiotherapy. *Int J Radiat Oncol Biol Phys* **65**: 924-933, 2006.
11) Nelson C, Starkschall G, Balter P, et al.: Respiration-correlated treatment delivery using feedback-guided breathhold: A technical study. *Med Phys* **32**: 175-181, 2005.

要旨：【目的】本研究の目的は，商用の呼吸同期照射システムで得た背腹方向の腹壁変位量とX線シミュレーターで観測した頭尾方向の肺腫瘍変位量の位相相関性を評価し，腹壁変位量が予測した腫瘍位置と測定した腫瘍位置のずれ量(以下，腫瘍位置ずれ量)を算出することであった．【方法】2006年12月から2008年3月までの間に，当院で肺定位放射線治療を施行した11症例を対象とした．そのうち6症例は倫理審査委員会の承認の下，3日間にわたって測定を行った．Real-time Positioning Managementシステム(Varian Medical Systems, Inc., Palo Alto, CA)で計測した腹壁変位量の画面と肺腫瘍変位量が投影されたX線シミュレーター(Acuity; Varian Medical Systems, Inc.)の画面を並列に表示し，自由呼吸下で60秒間計測した．取得した並列画像に対して画像処理を行った後，テンプレートマッチングで肺腫瘍の位置を検出した．腹壁変位量と肺腫瘍変位量から位相相関性を評価した．また，位相ずれを補正した回帰直線を用いて，腹壁運動が予測した肺腫瘍位置を求め，これと測定した肺腫瘍位置を比較することで，腫瘍位置ずれ量を算出した．【結果】相関係数の絶対値は0.89から0.97の範囲内にあり，これらの日々の変動も安定していた．腹壁変位量と肺腫瘍変位量の位相ずれが原因で生じるヒステリシス曲線を描く症例も存在した．腫瘍位置ずれ量の平均値は最大で1.78mmであった．【結論】多くの症例で，腹壁変位量と肺腫瘍変位量との位相相関性は良好であったが，腹壁変位量が予測した肺腫瘍位置と測定した肺腫瘍位置の間にずれが生じていた．